Extracting Green's functions from random noise and vibrations

IRA DYER SYMPOSIUM

MIT

June 14, 2007

W. A. Kuperman

Scripps Institution of Oceanography

wkuperman@ucsd.edu

OUTLINE

- INTRODUCTION
- UNDERWATER ACOUSTICS NOISE:
  - THEORY
  - EXPERIMENT
- SIGNAL PROCESSING (Sync and AEL or Arrays)
- SEISMOLOGY
- Other APPLICATIONS
  - STRUCTURAL ACOUSTICS
  - HUMAN BODY NOISE
- CONCLUDING REMARKS

Green's Functions Estimate from "Noise"
Background Theory and Data Realizations

– **Ultrasonics diffuse wavefields (~1MHz)**
  - **Lobkis and Weaver (Phys. Rev. Lett. , 2001),** Derode et al. (JASA 2003), Larose et al. (JASA 2004), Malcolm et al. (*Phy. Rev. E.* 2004)

– **Structural Engineering (~1kHz)**

Farrar et al. (1997), Larose et al. (JASA 2006), Sabra et al. (JASA 2006)

– **Ocean ambient noise (~100Hz)**
  - **Roux and Kuperman (JASA, 2004),** Roux et al. (JASA 2005), Sabra et al. (JASA, 2005)

– **Seismic ambient noise (<1HZ)**
  - Aki (1957), Claerbout (Geophys. J. Int. 1968), **Shapiro and Campillo** (G.R.L., 2004, **Science 2005),** Snieder (*Phy. Rev. E.* 2004), Wapenaar et al. (Geophys. J. Int. 2004), Schuster et al. (Geophys. J. Int. 2004), **Sabra et al. (G.R.L., 2005)**

– **Helioseismology**
  - Duvall et al. (Nature, 1993), Claerbout & Rickett, (The Leading Edge 1999).

-- **Human Body Noise:** Sabra et al, A. Phys. Lttrs (2007)

Applications exist in a wide range of environments and frequency bandwidths because the physics driving this noise cross-correlation process remains similar.

Coherent signals from noise data

First experimental demonstration in ultrasonics (0.1 – 0.9 MHz)

R.L. Weaver & O.I. Lobkis, Phys. Rev. Lett., 2001

“By cross-correlating ambient noise recorded at two locations, the Green’s function between these two locations can be reconstructed”. (J. Claerbout 1999, R. Weaver 2001.)

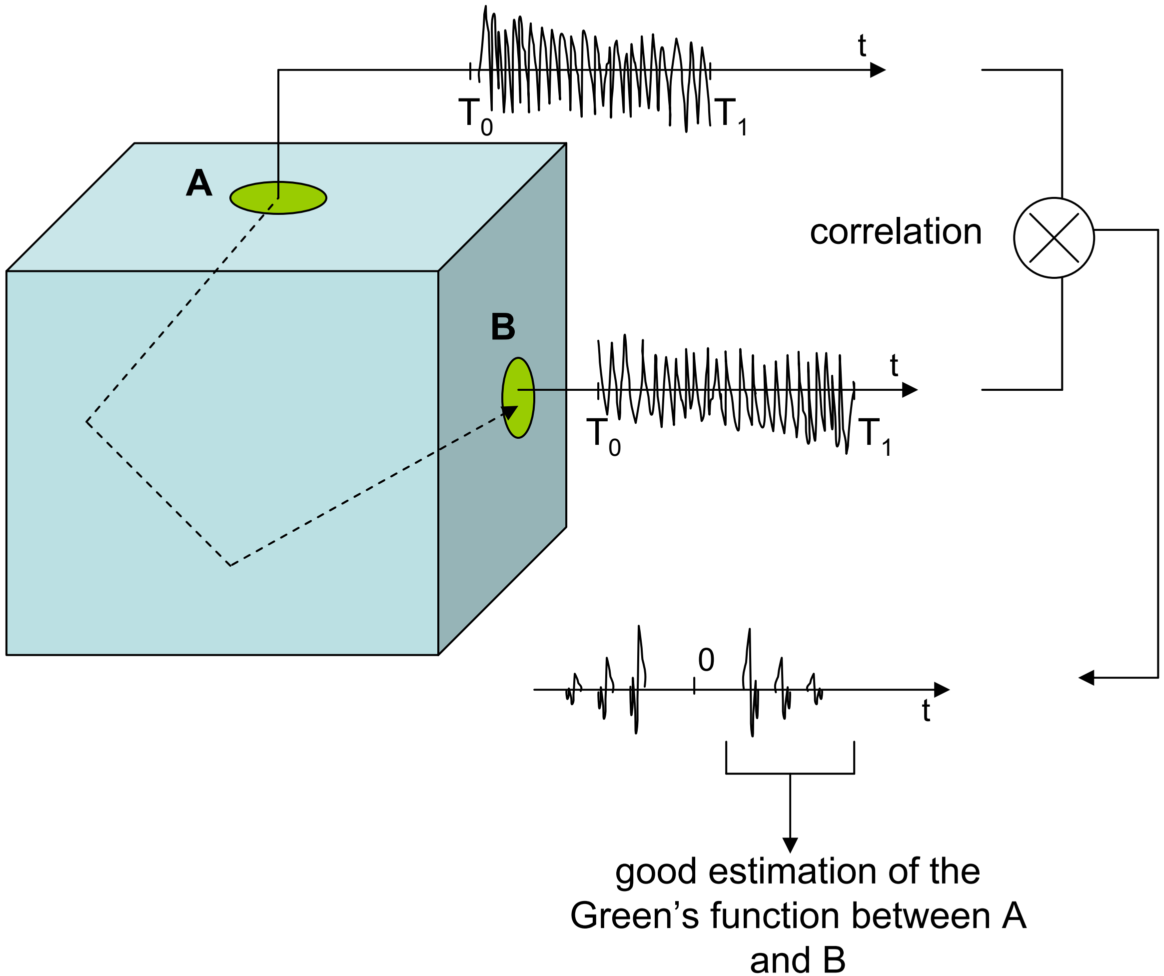

HOW COME WEAVER CAN USE WHITE NOISE AND WE CAN'T?

From array point of view: White noise is non-travelling, independent, unrelated noise hanging around each individual sensor.

ONE MAN'S WHITE NOISE…

CORRELATED

Weaver et al

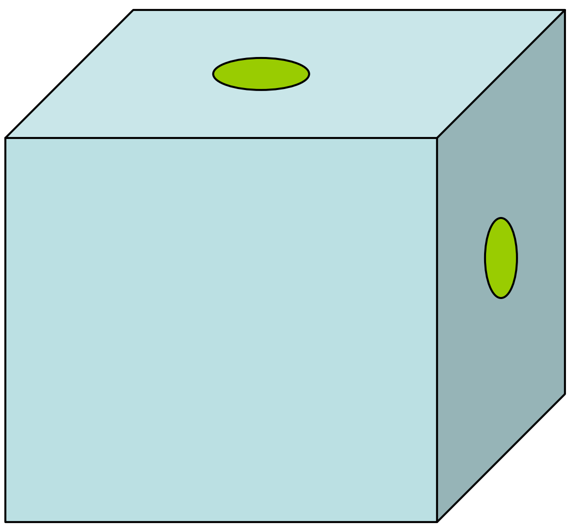

ARRAY

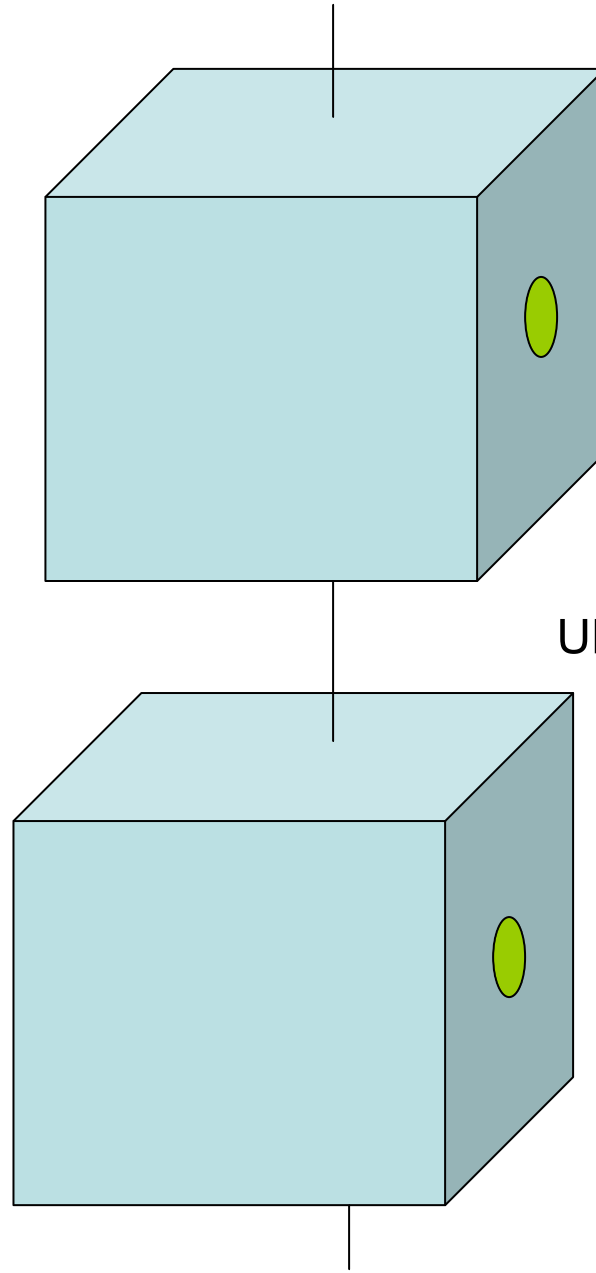

UNCORRELATED

SENSOR NOISE

Noise cross-correlation: Free space

$$C_{12}(\tau) = \int_{-\infty}^{\infty} P(\mathbf{r}_1, t)\, P(\mathbf{r}_2, t+\tau)\,\mathrm{d}\,t.$$

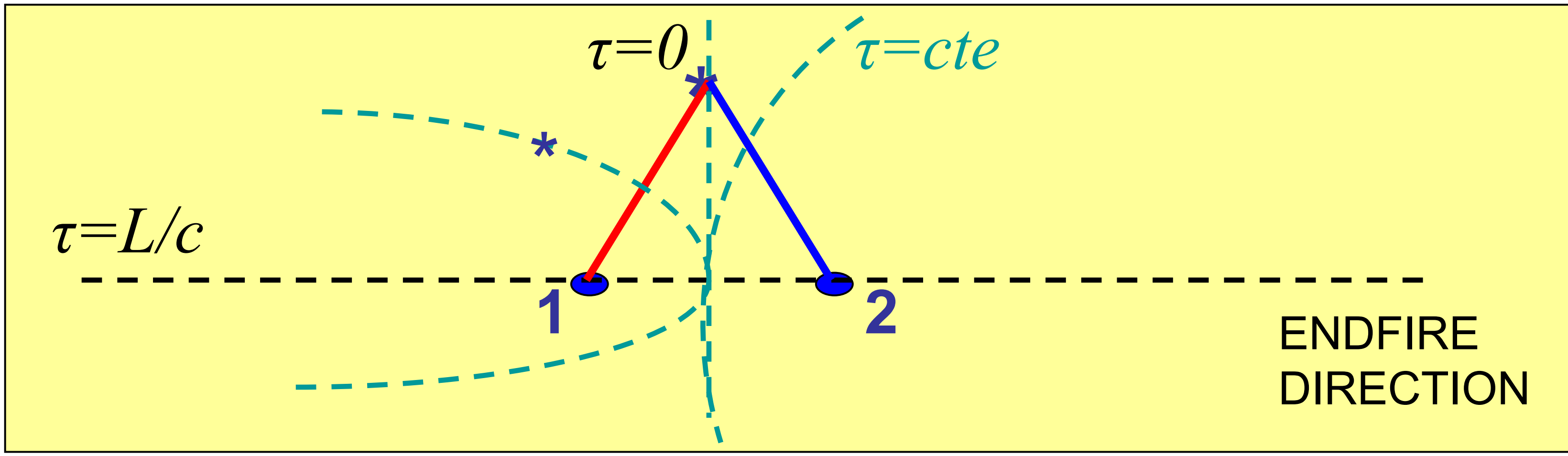

Noise sources yielding constant time-delay τ, lay on same Hyperbola

$$\tau = \frac{\left|\boldsymbol{r}_2 - \boldsymbol{r}_s\right| - \left|\boldsymbol{r}_1 - \boldsymbol{r}_s\right|}{c} \leq \frac{L}{c}$$

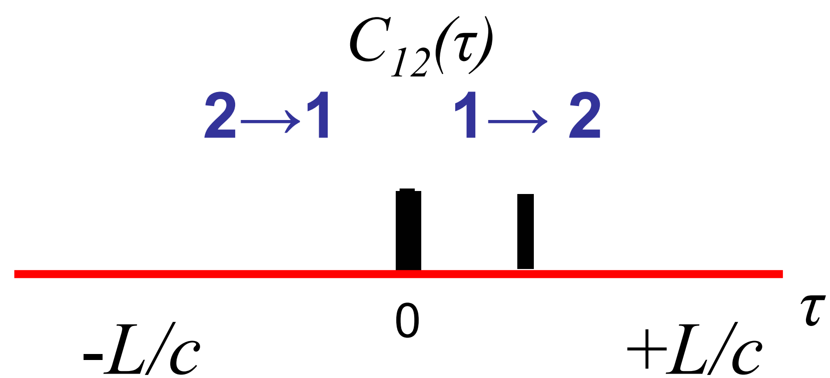

Isotropic distribution of uncorrelated random noise sources

C, dC/dt, band-limited signal

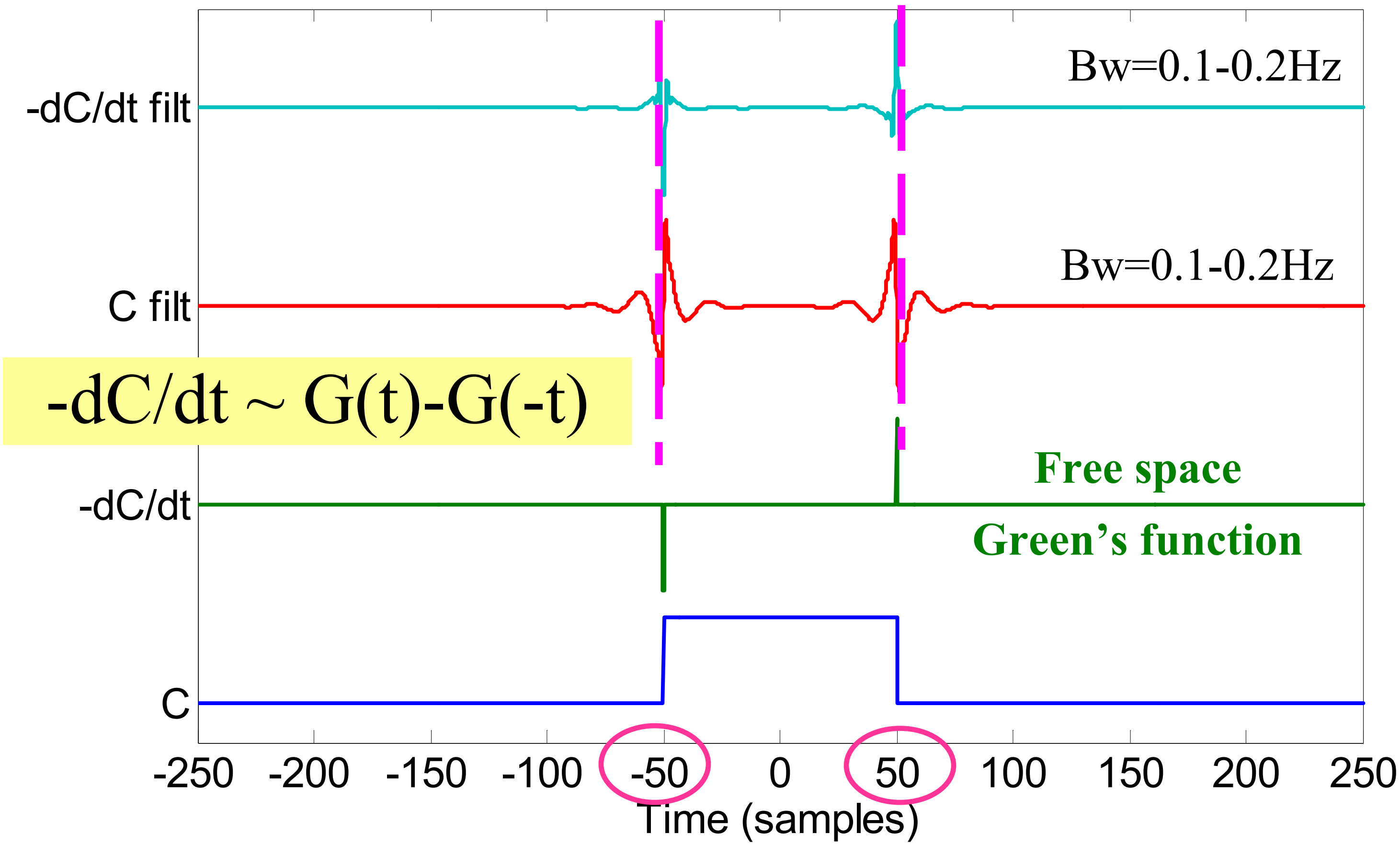

•With cross-correlation process the phase of the source signal is removed,

→Arrival time is given by the center of the pulse (envelope maximum)

•Isotropic noise distribution → Symmetric Correlation function.

Underwater Acoustics

(non-free space)

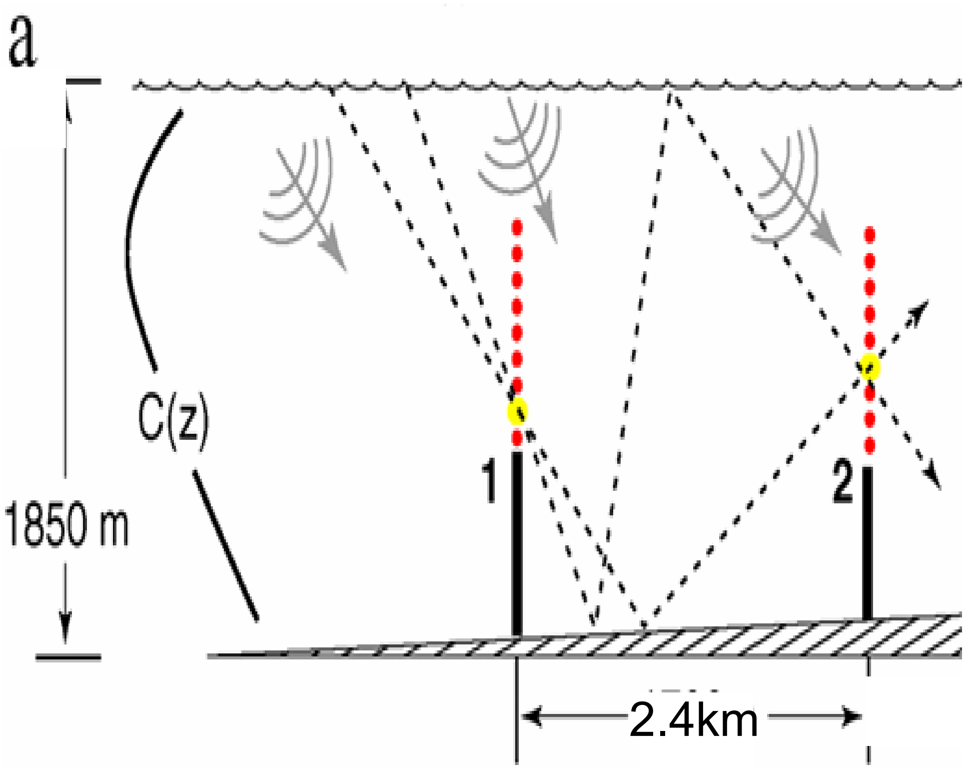

Experimental results (70 – 130 Hz)

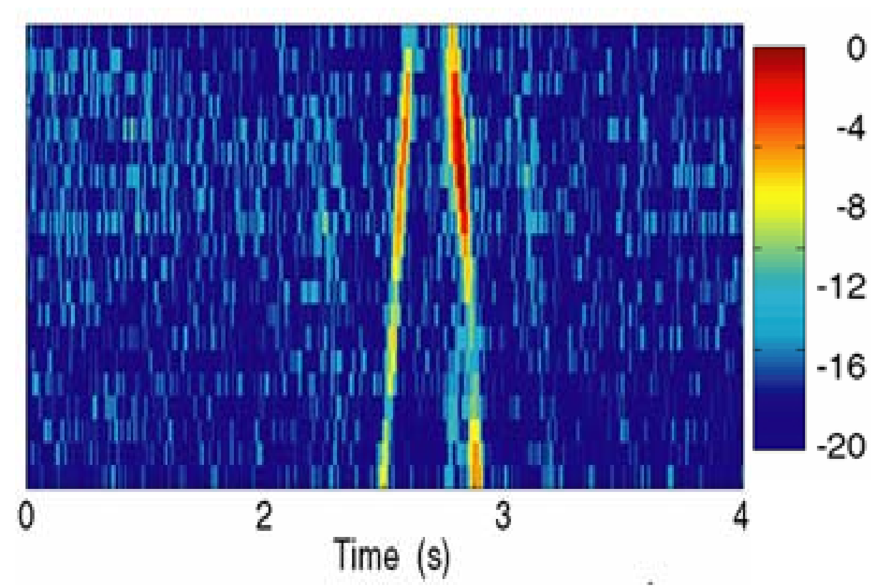

Noise events propagating through receivers 1 and 2 average-up coherently over the long-time in the cross-correlation function.

Coherent wavefronts yield an estimate of the Green's function between 1 and 2.

Roux & Kuperman (JASA, 2004), Sabra et al. (JASA, 2005), (IEEE. J. Ocean. Eng. 2005)

Experimental results (70 – 130 Hz)

NPAL experiment

(Worcester et al)

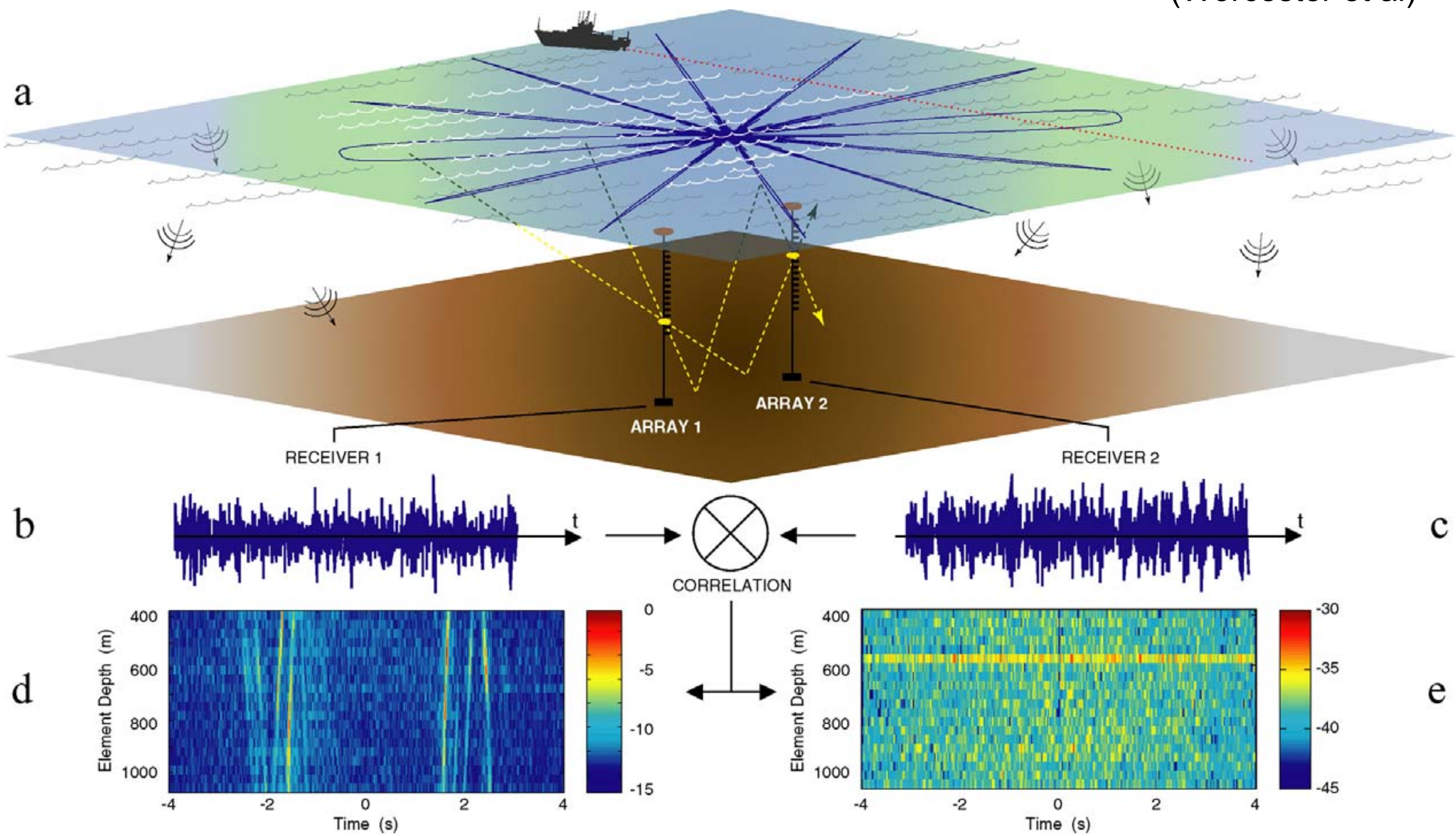

Experimental results (70 – 130 Hz)

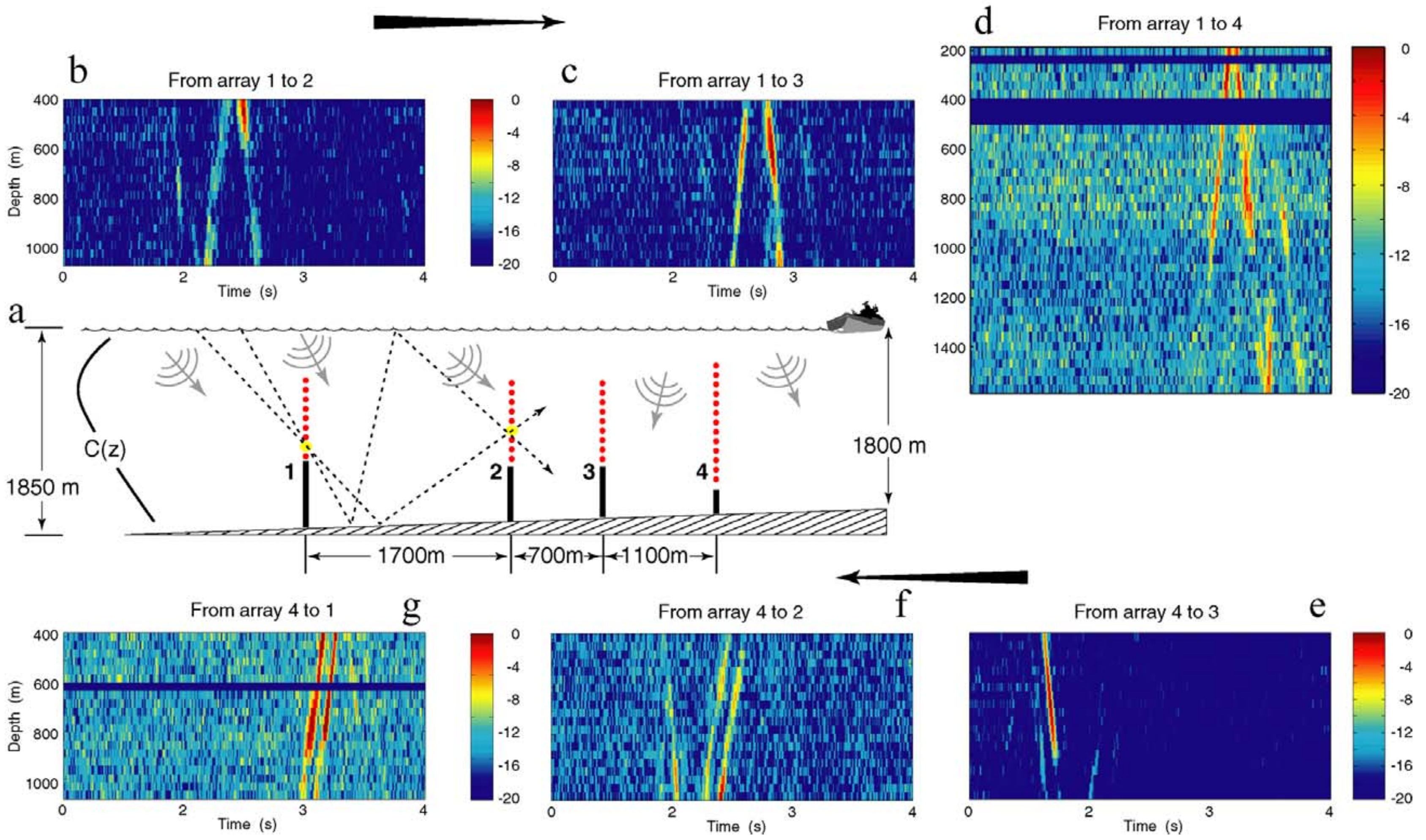

Time reversal using noise as a probe source (70 – 130 Hz) [2->3]

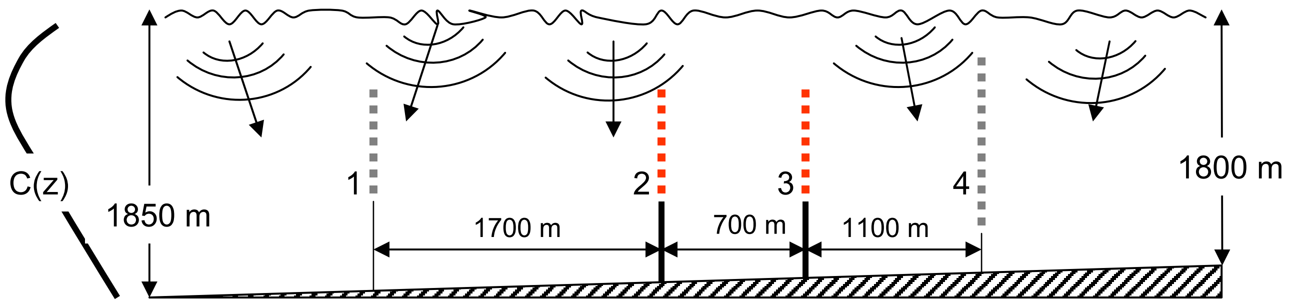

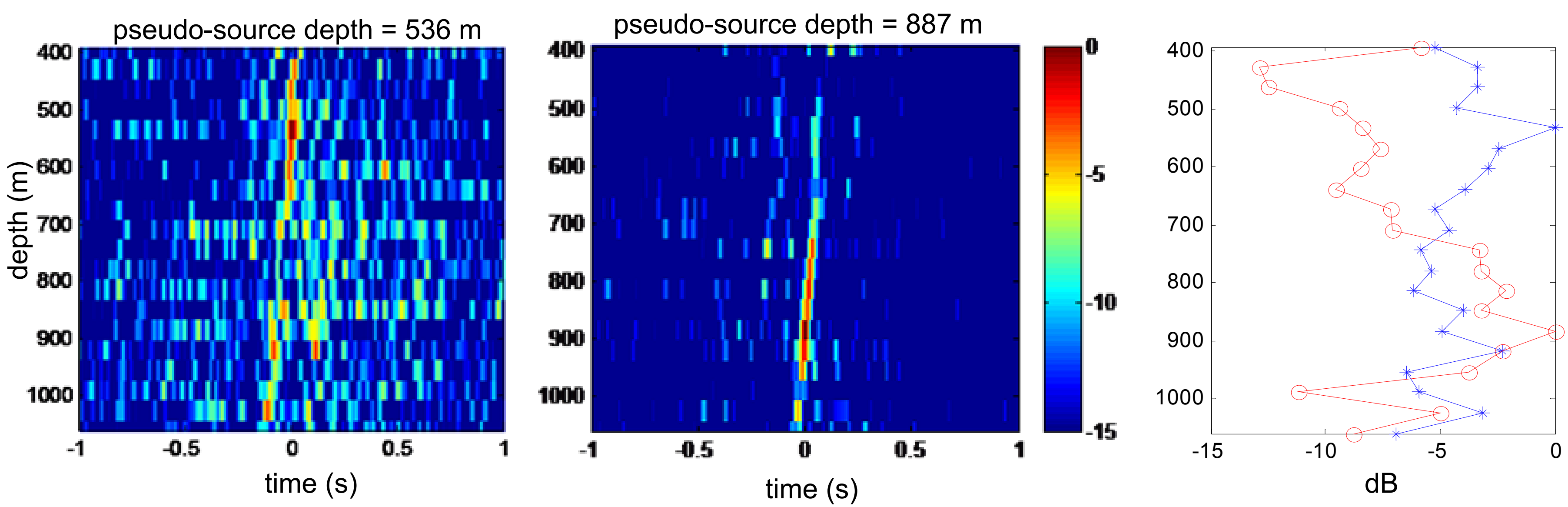

Time reversal using noise as a probe source (70 – 130 Hz) [4->3]

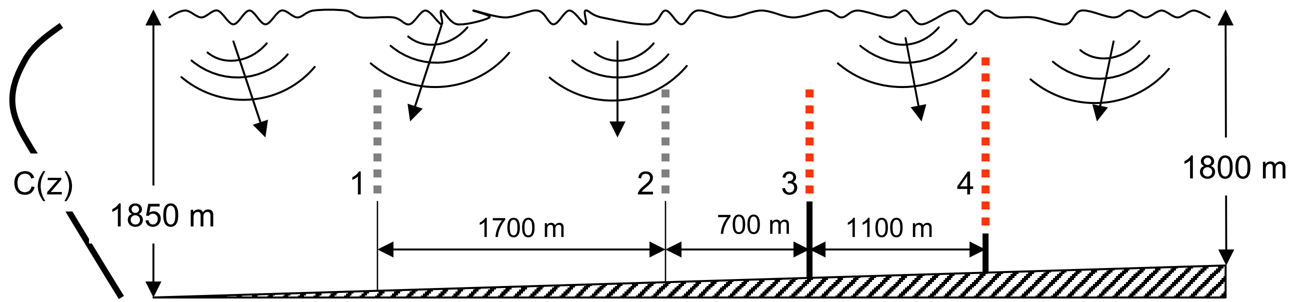

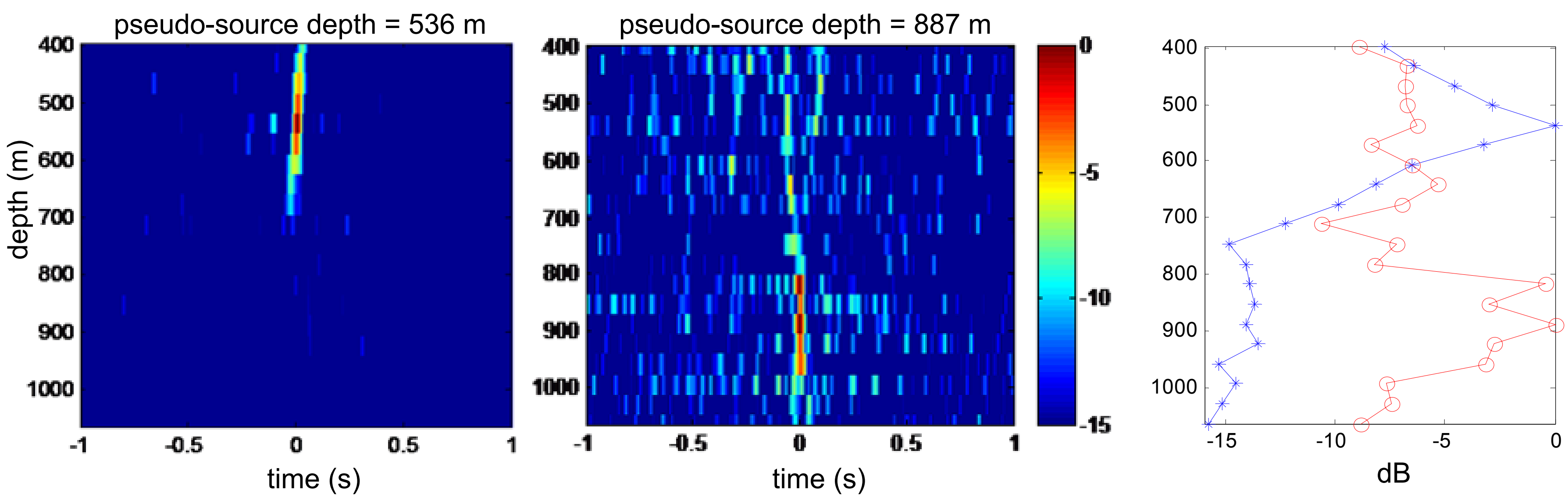

Time reversal using noise as a probe source (70 – 130 Hz) [2&4->3]

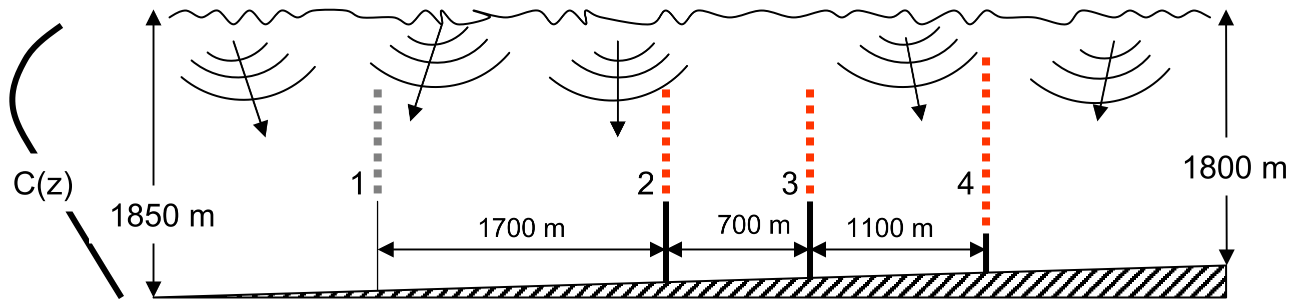

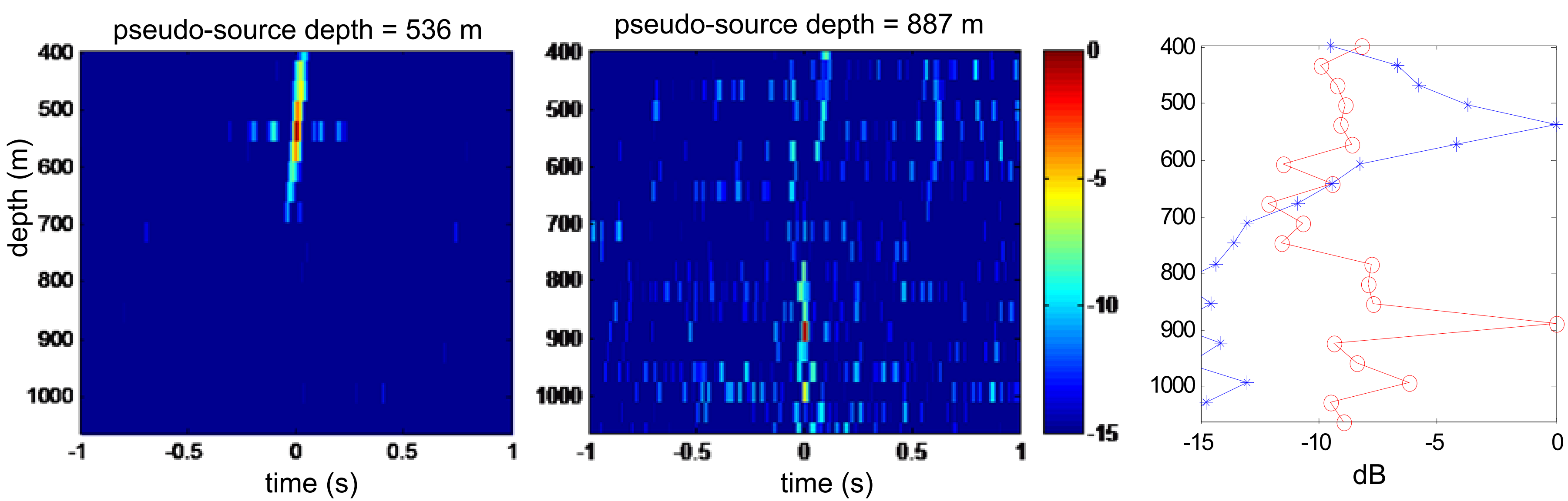

VERY RECENT APPLICATION

A passive fathometer and sub-bottom profiler using ambient noise

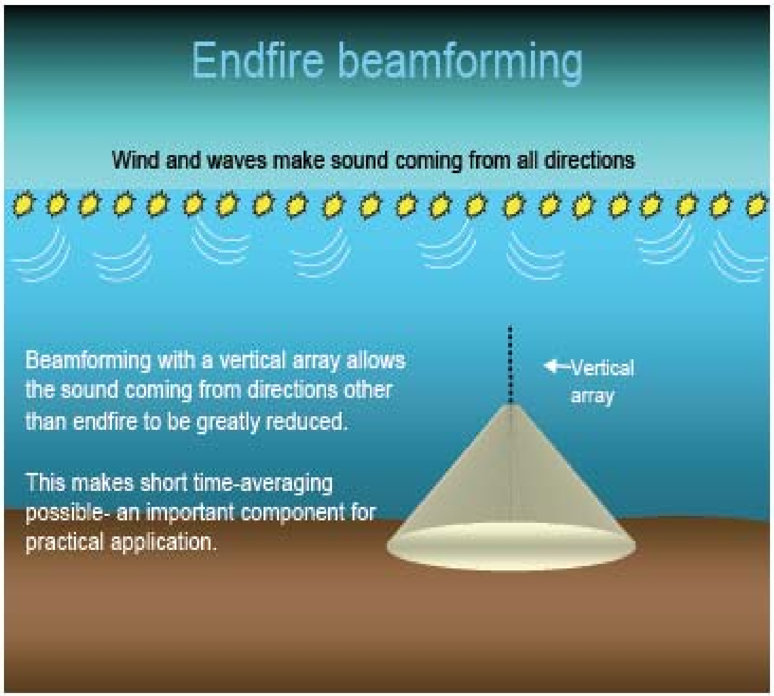

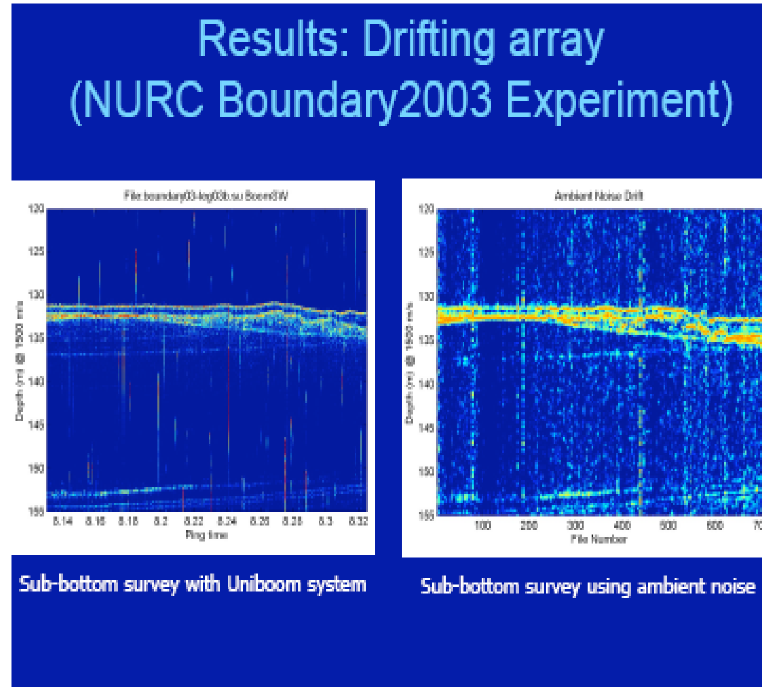

Siderius, Harrison and Porter In JASA

Adaptive beamforming

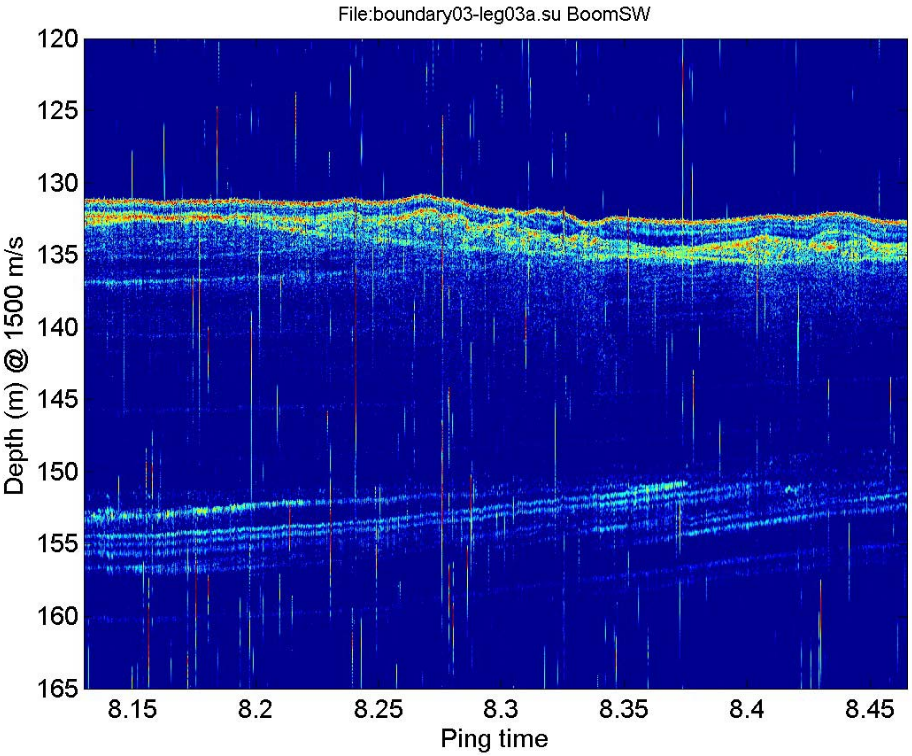

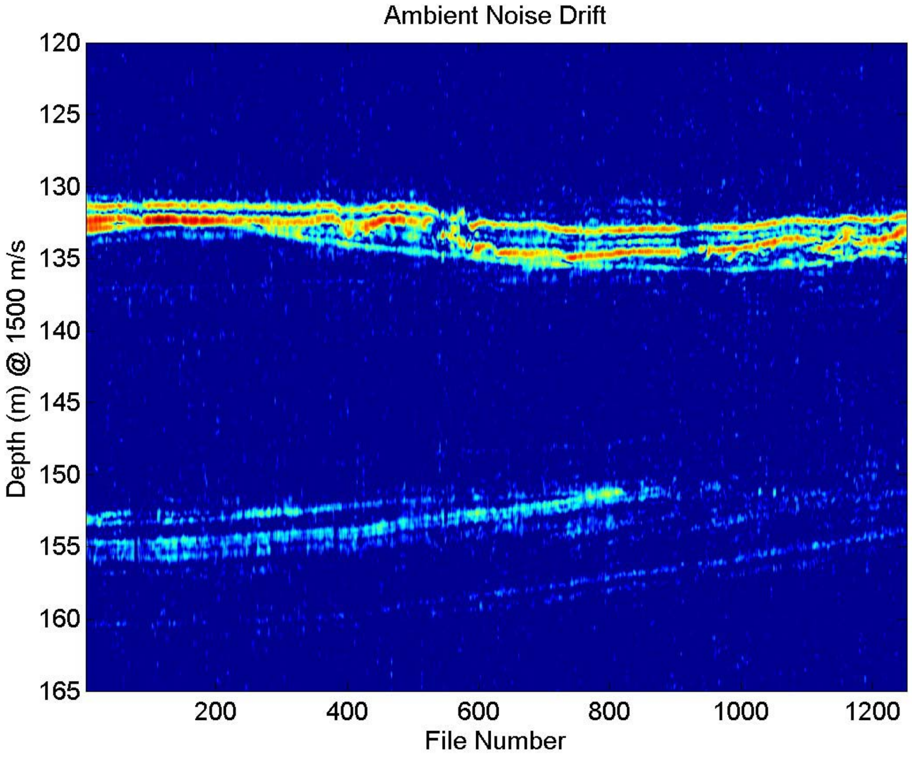

Sub-bottom survey with Uniboom system

Sub-bottom survey using ambient noise and adaptive beamforming

Siderius,Harrisonand Porter

Experimental Set-Up

- Adaptive Beach Monitoring experiment (ABM 95) Spring 95. South Calif.
- 2 bottom arrays were, 3.4km offshore, H= 21m of water
- 4m very fine sand sediment layer, high attenuation. Sandstone basement

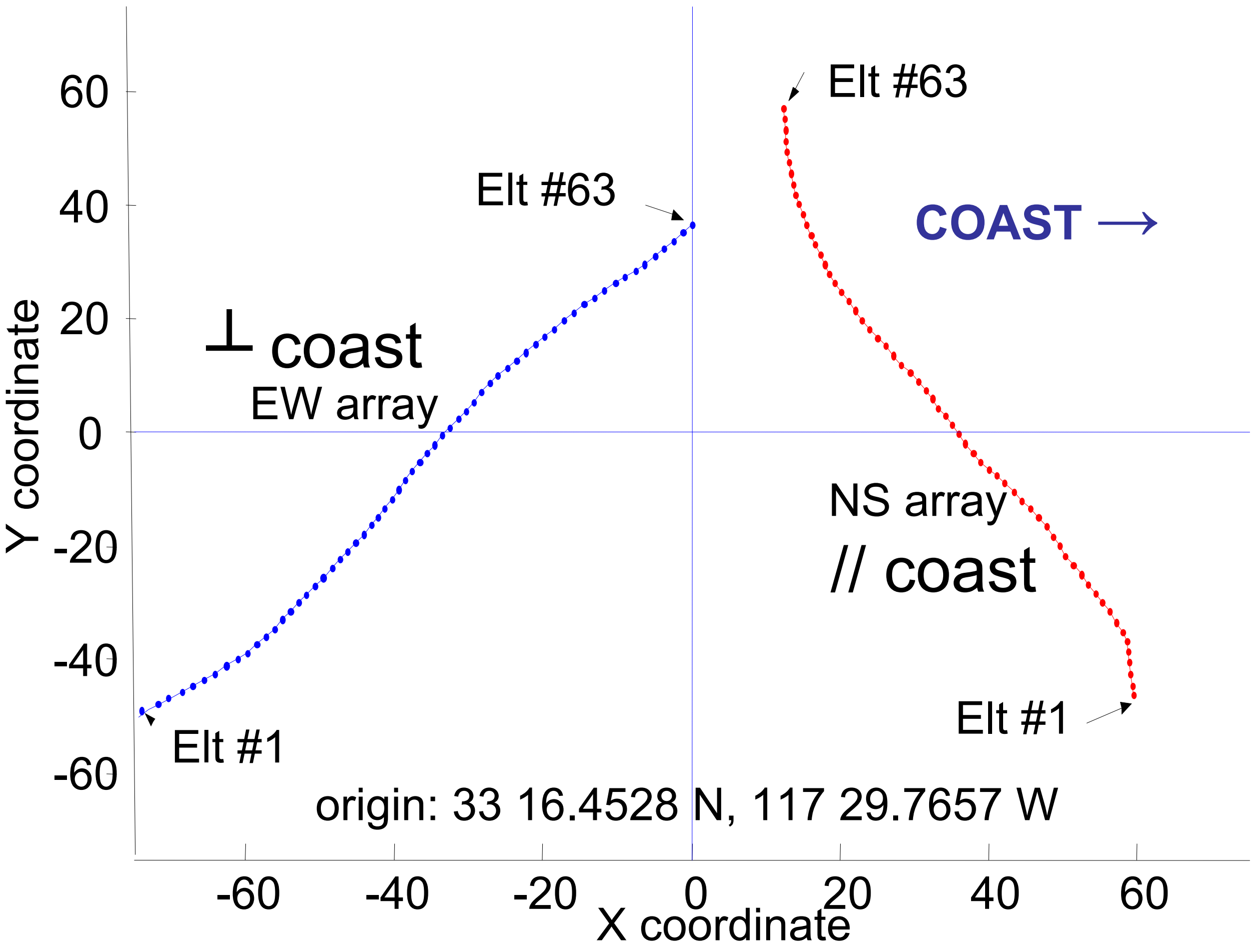

- 64 elements (D_{max}=1.875m~λ/2 @ 400Hz)
- Bandwidth: [2Hz-750Hz]. Flat response
- F_S=1500 Hz.
- 2 weeks continuous recordings of ambient noise

Motivation

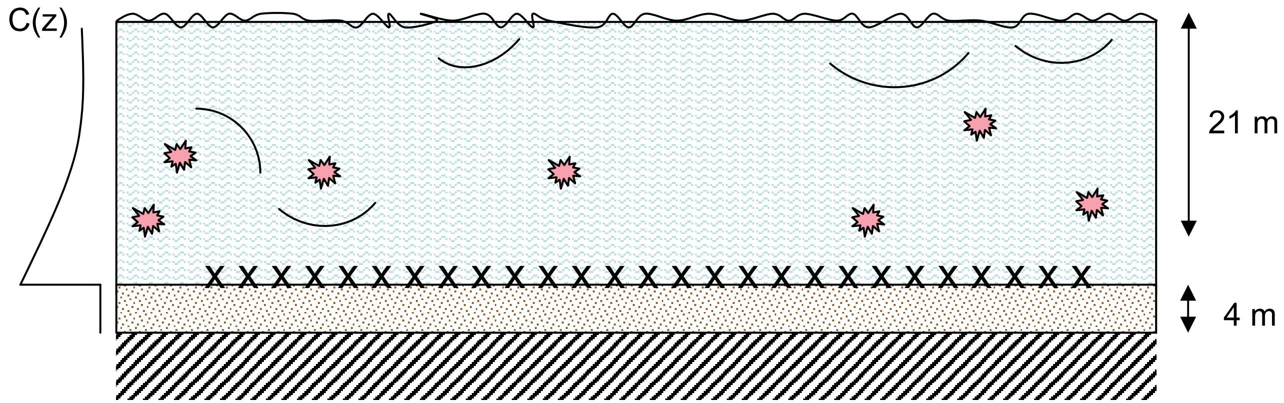

Determine environmental characteristics from cross-correlation of ambient-noise recordings along a horizontal array.

Ambient-noise NCF

Time-derivative of the NCF. NS array, Elt 30-45. Symmetry w.r.t to time origin

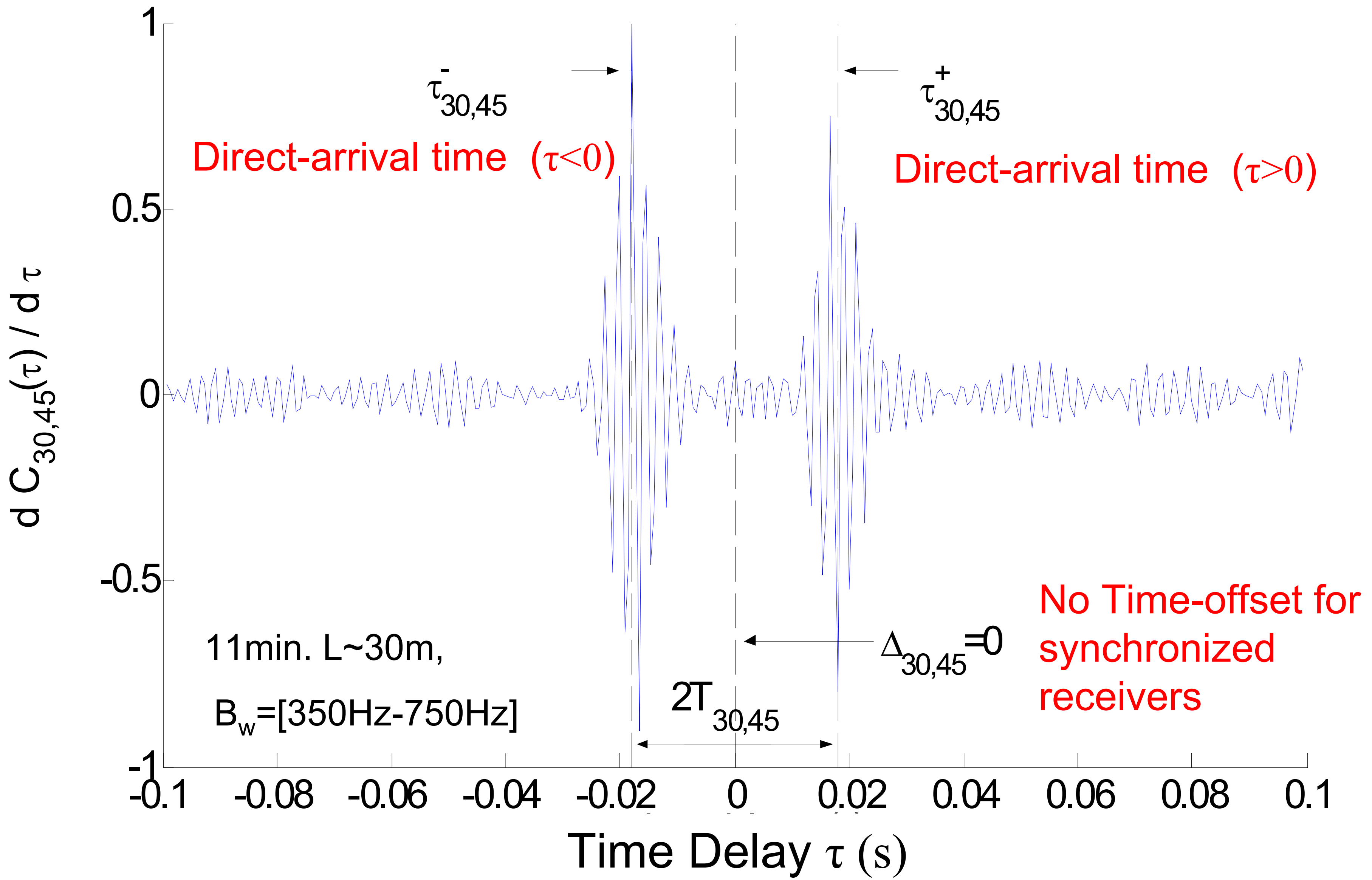

Horizontal Coherent Wavefronts

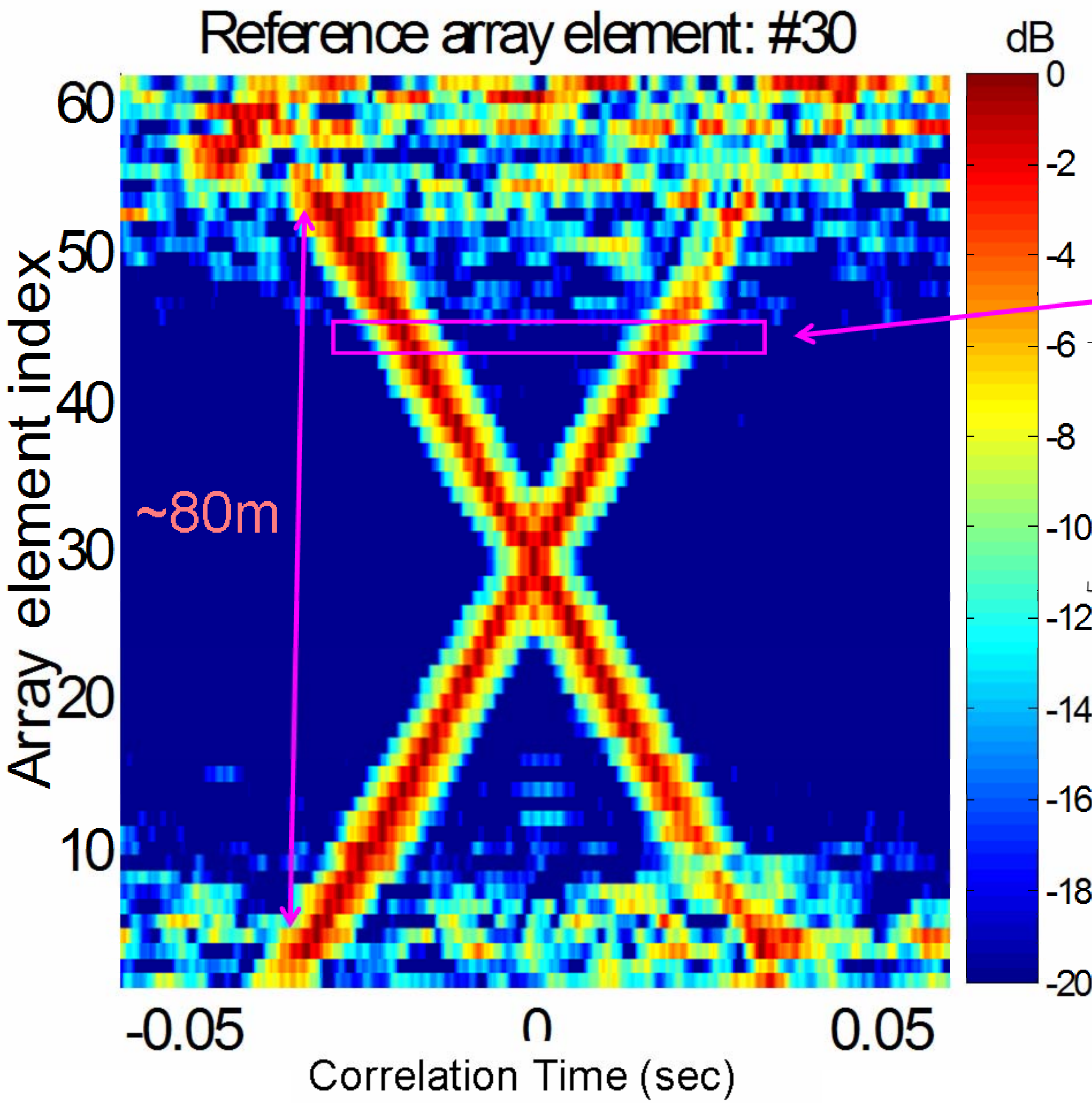

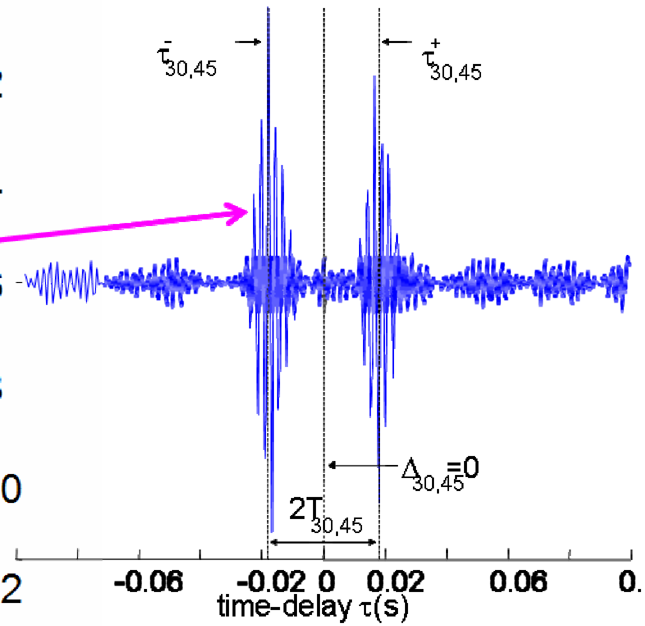

JD 151, 5.26. AM (GMT).

11 min Data.
Bw=[350Hz-700Hz]

Array Element Self-Localization

- Non linear Least Square Inversion (2D+c_0) for AEL.
- A-priori information: Dmax=1.875m. Minimize array curvature.

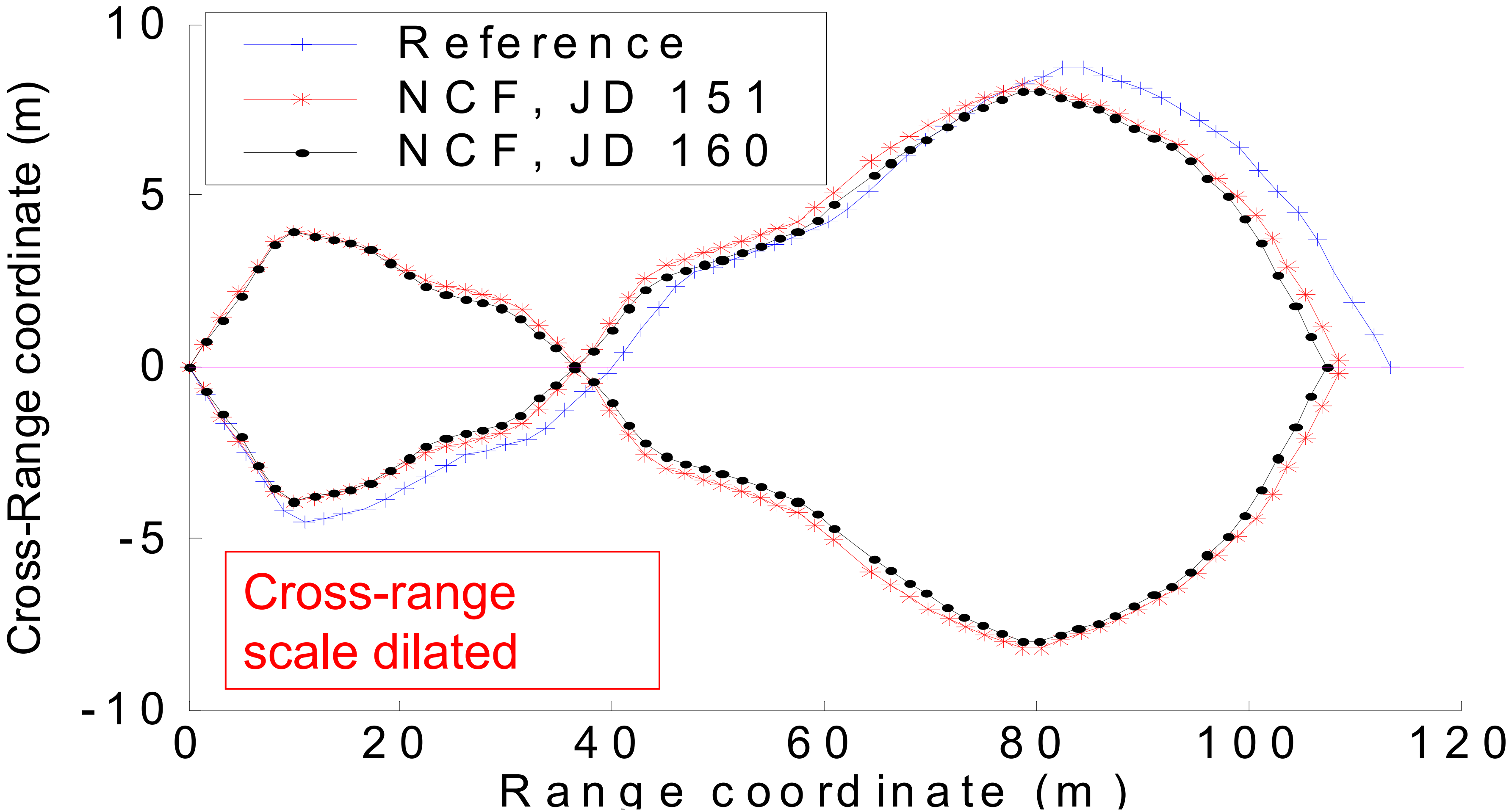

JD 151 c_0=1490m/s, RMS Error~0.40m

JD 160 c_0=1485m/s, RMS Error~0.43m

Towed Source Beamforming

AEL from JD 151 c0=1490m/s. Plane wave beamforming. CSDM with 5sec FFT.

N=63 Elts; 20log N ~36dB

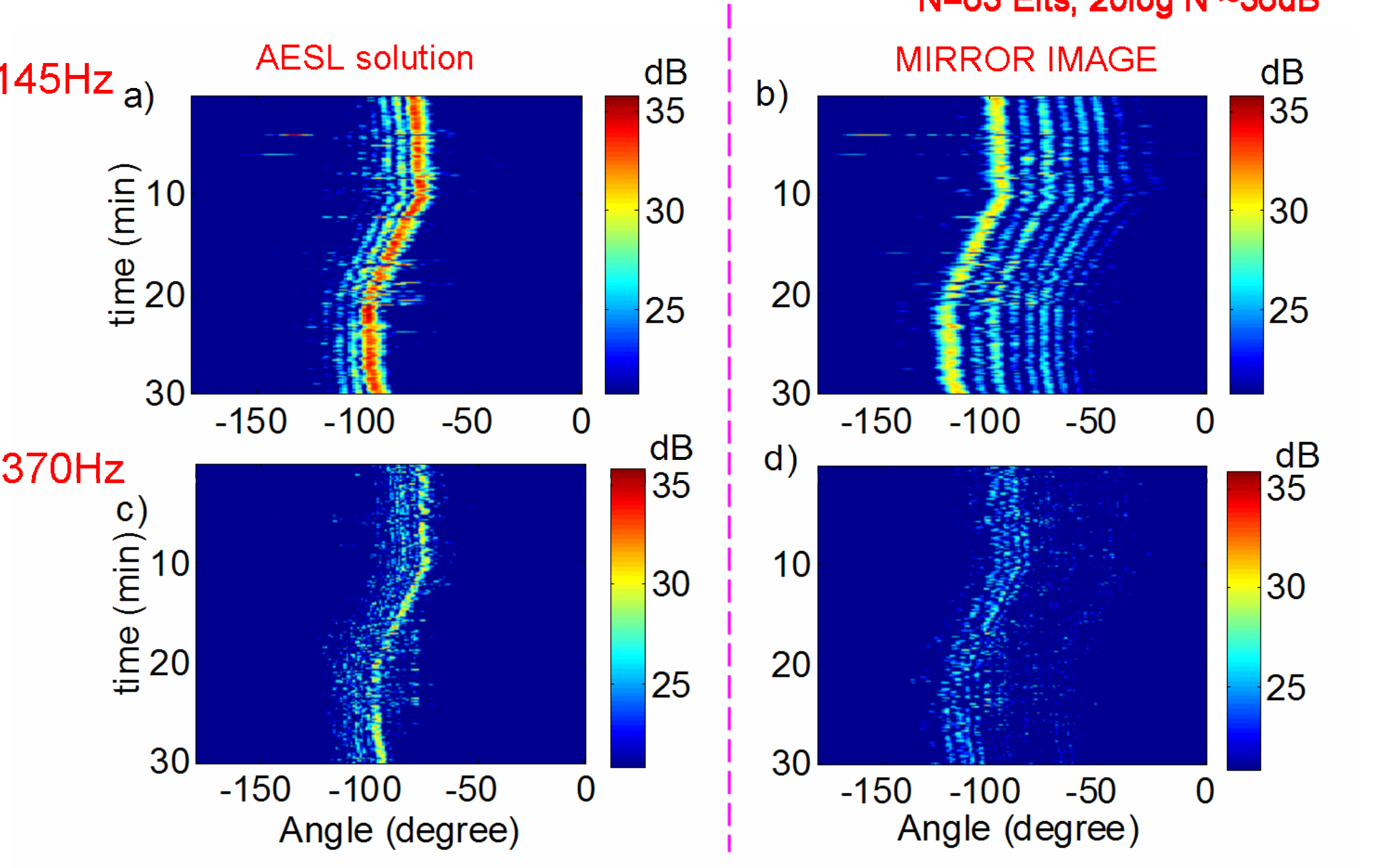

Array Element Self-Synchronization

Time-derivative of the NCF. NS &EW array, Elt 63 →Time-shifted origin

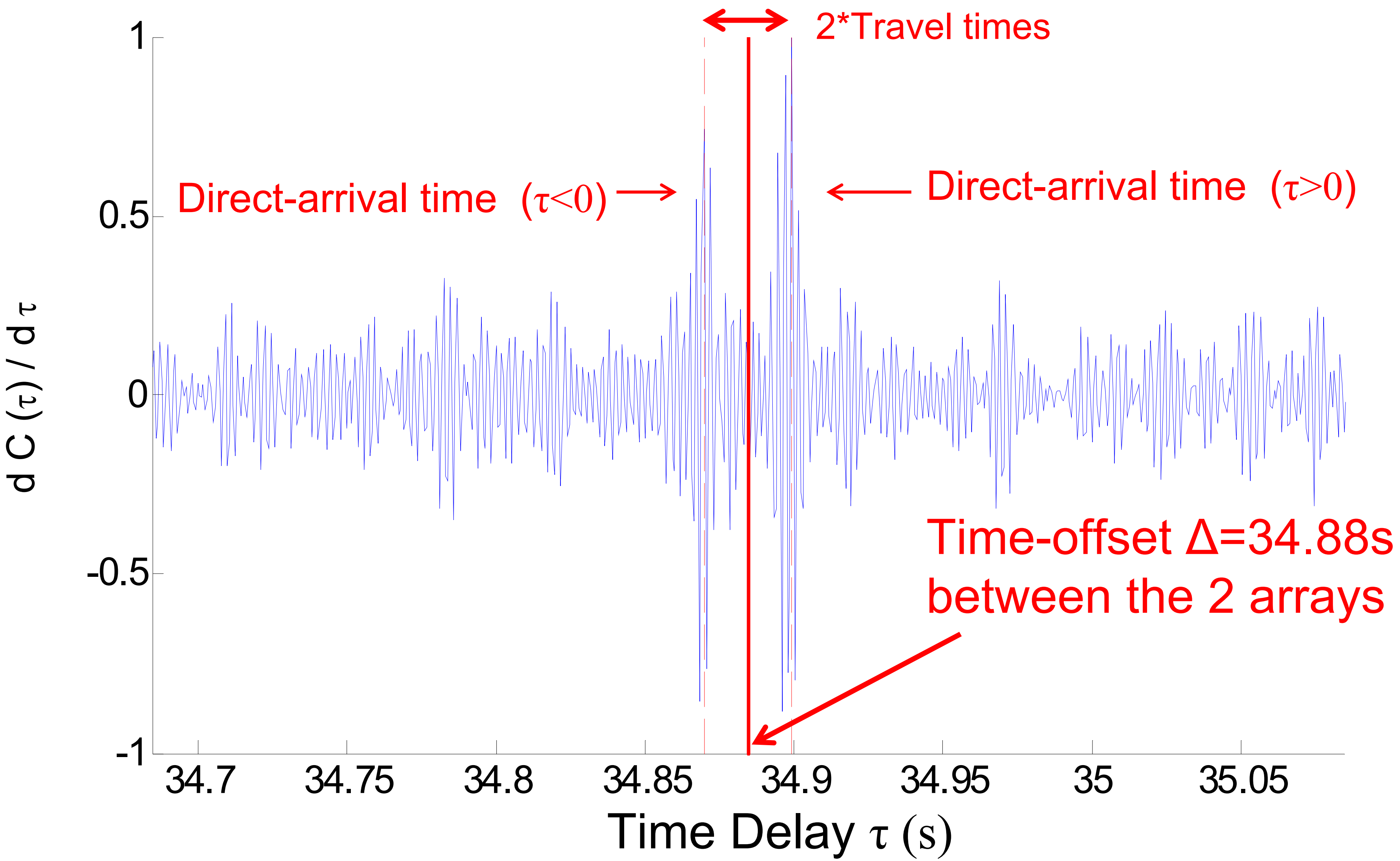

NCF traces (Data)

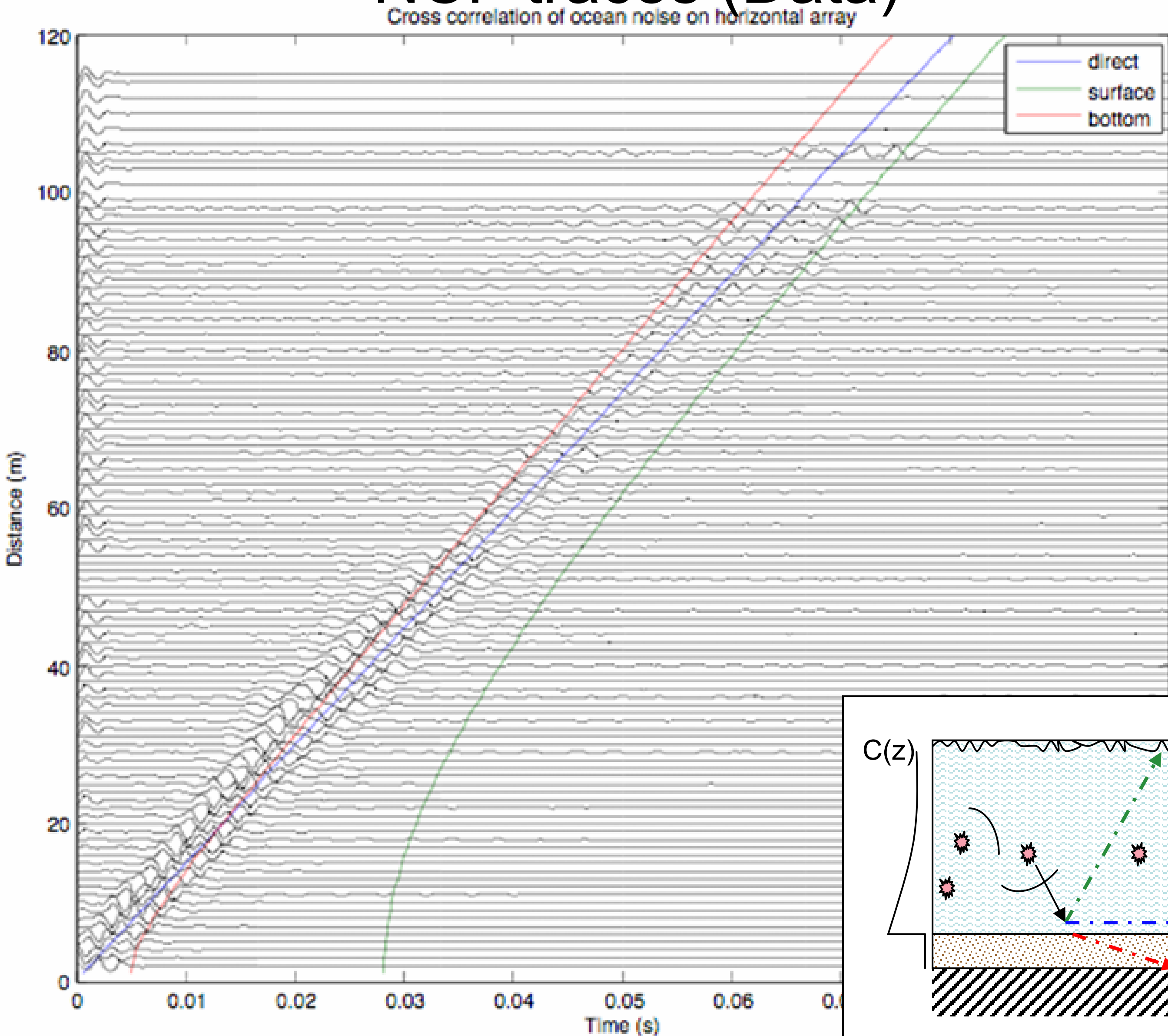

-NCF stacked by separation distance of receivers.

- Colored lines represent simplified isovelocity description of propagation paths.

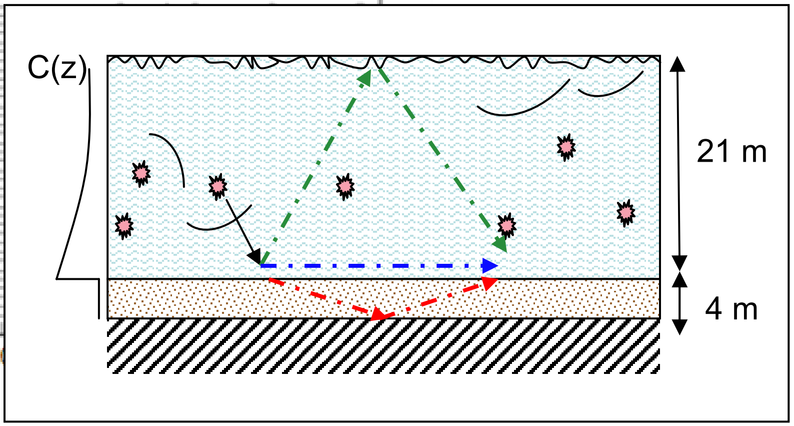

Stephanie Fried

Compare NCF & Simulation

NCF of data

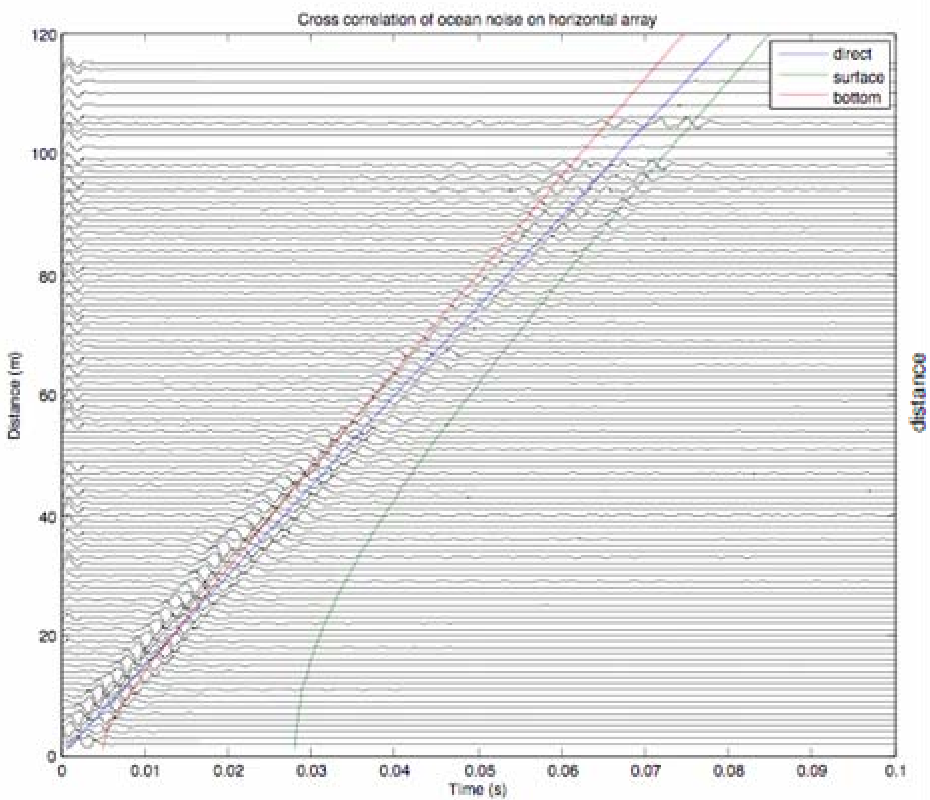

Spectral simulation of Green's fnc

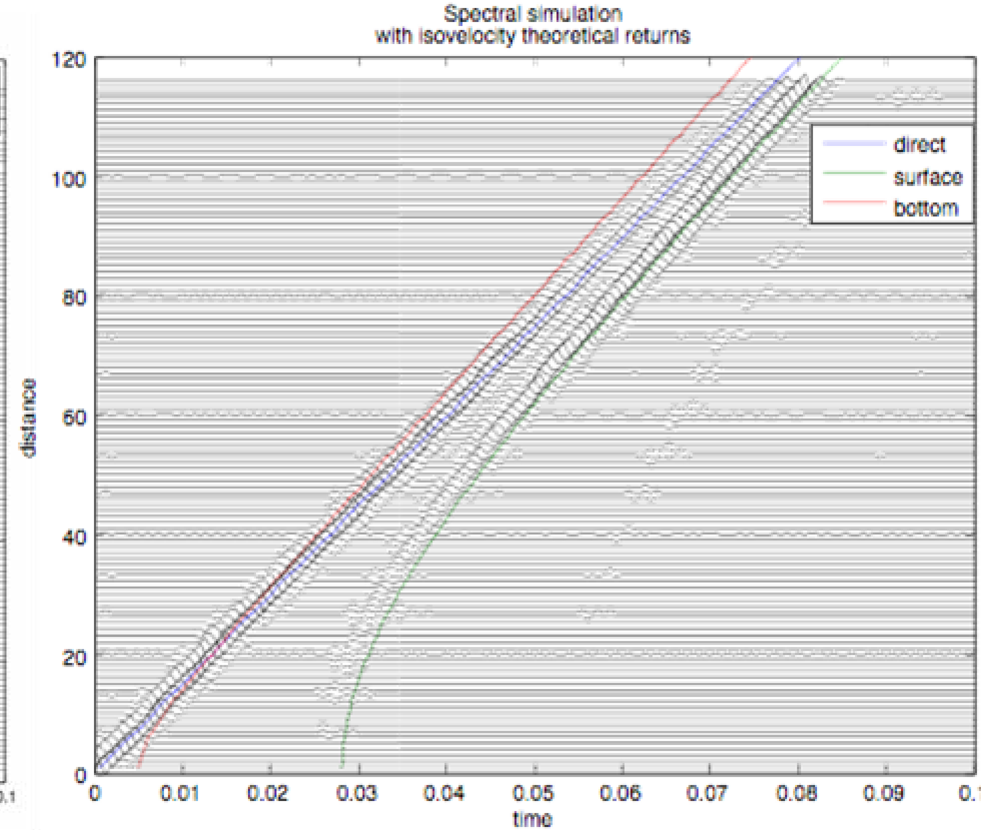

Stephanie Fried

High resolution surface wave tomography from ocean microseisms in Southern California

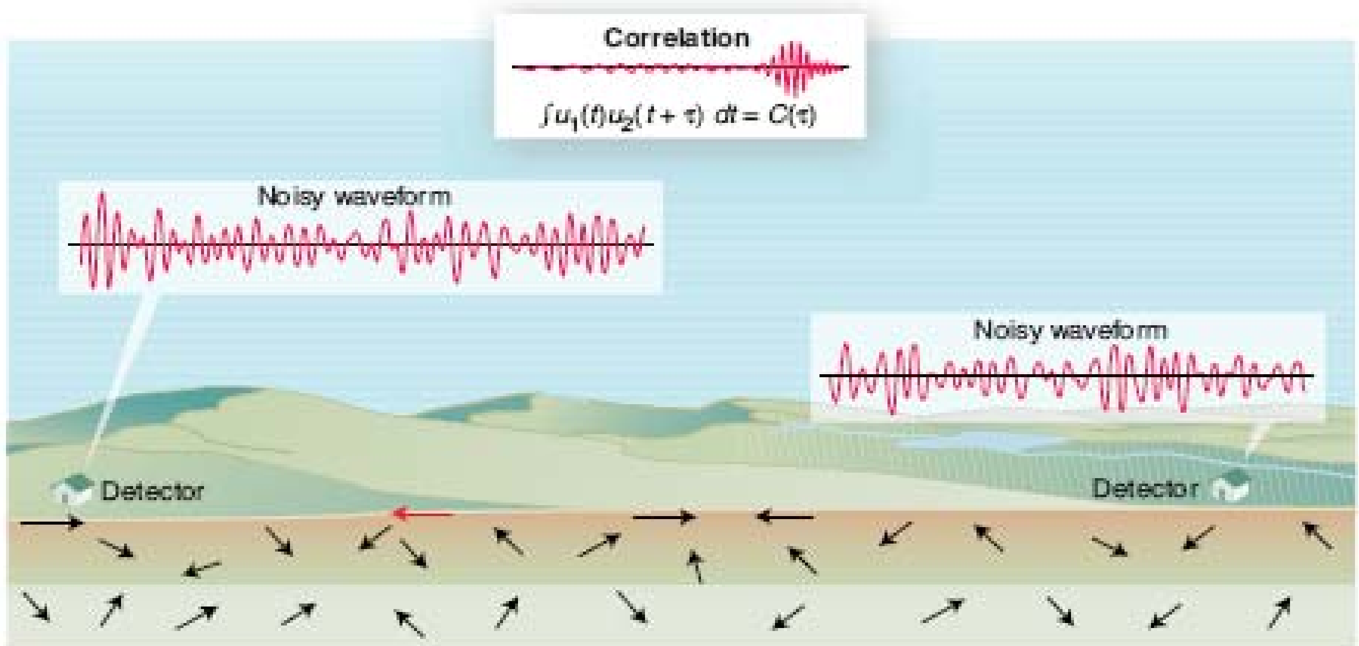

Vertical Component

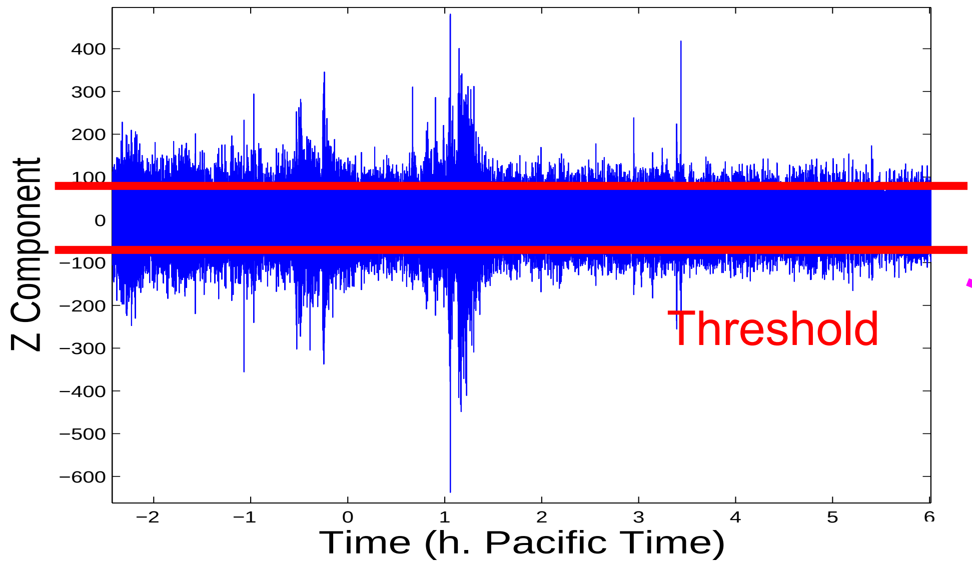

Station Location

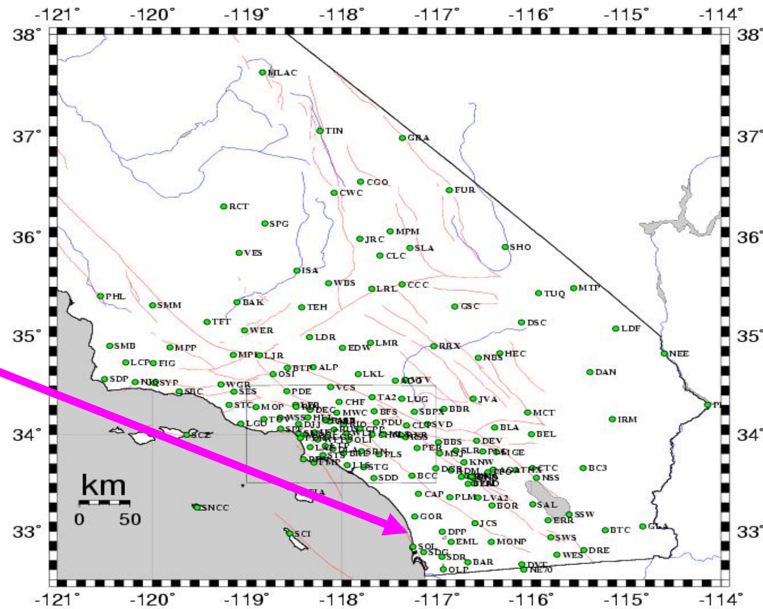

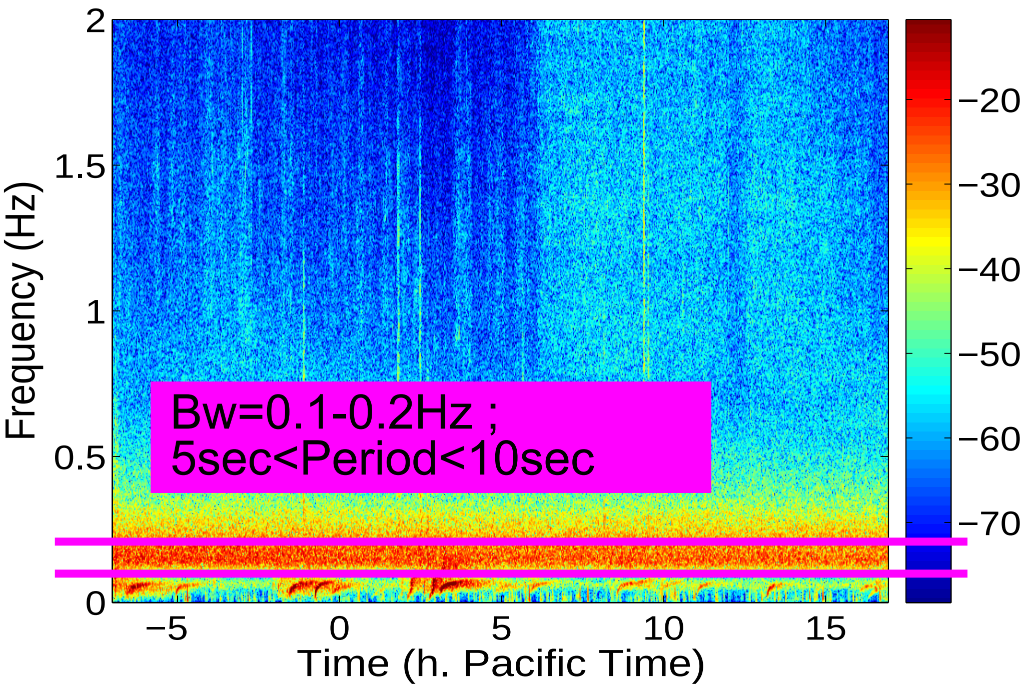

Southern California Seismic Network
(150 Stations)
Broadband data. Fs=10Hz.
18 Days of continuous data

Ocean microseisms propagate mainly as Rayleigh waves

Emergence rate of coherent waveforms

B_w=[0.1-0.2Hz], Z-comp. R=150 km

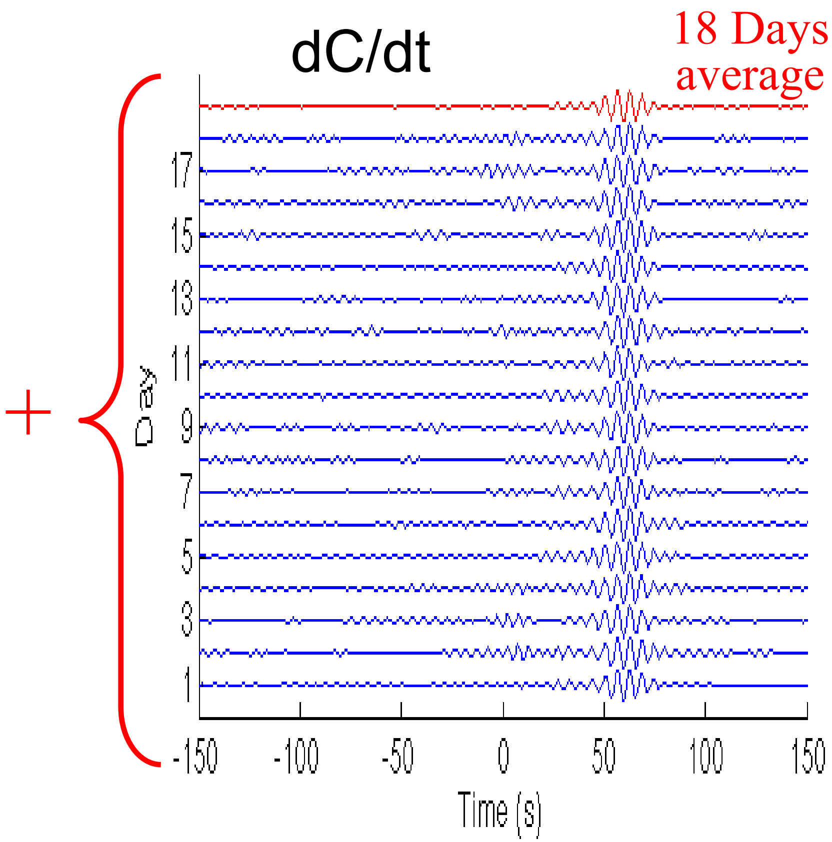

$$SNR = \max(Trace) / std(Trace)_{\tau > 150s}$$

$$SNR \propto \sqrt{T_r B_\omega}$$

“Passive Shot Gather”.

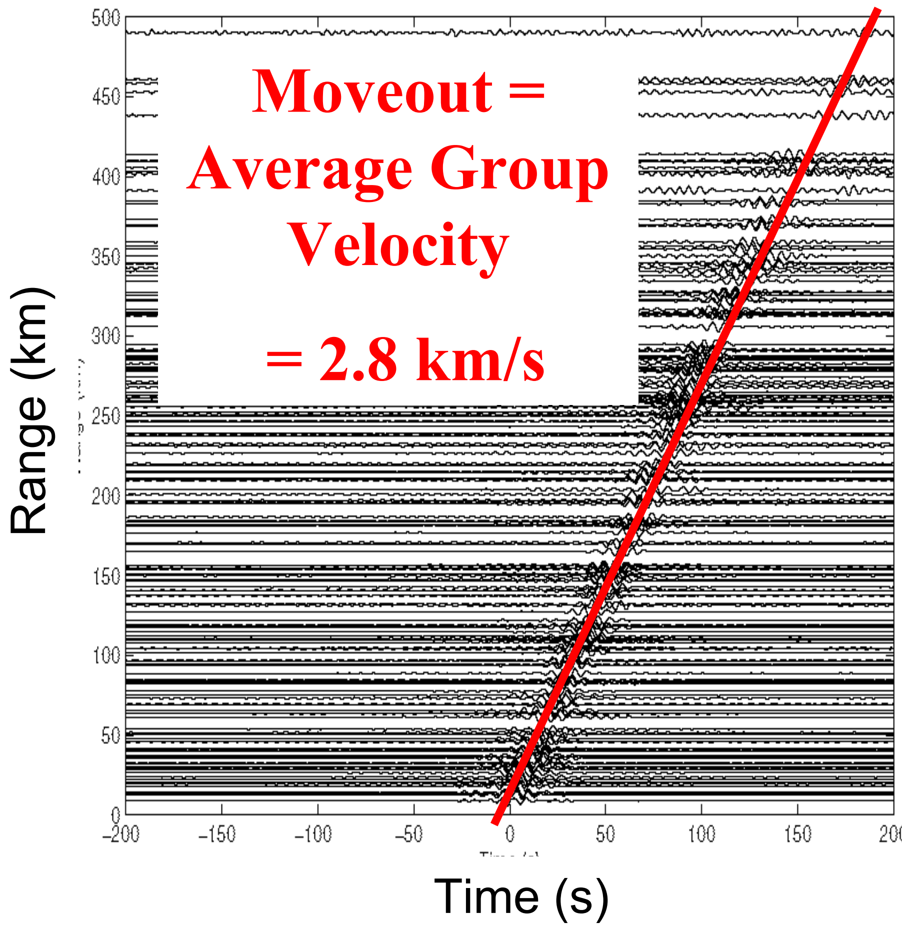

Station Pair (oriented 0° -21° North)
i.e. perpendicular to the coastline
(directionality of the ocean microseisms)

Spatial resolution & stationary phase

Stationary

Phase

Lobes

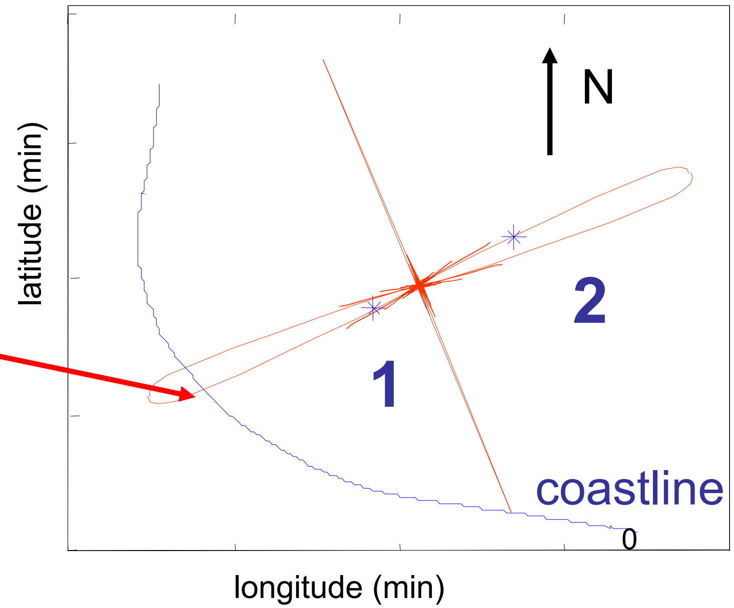

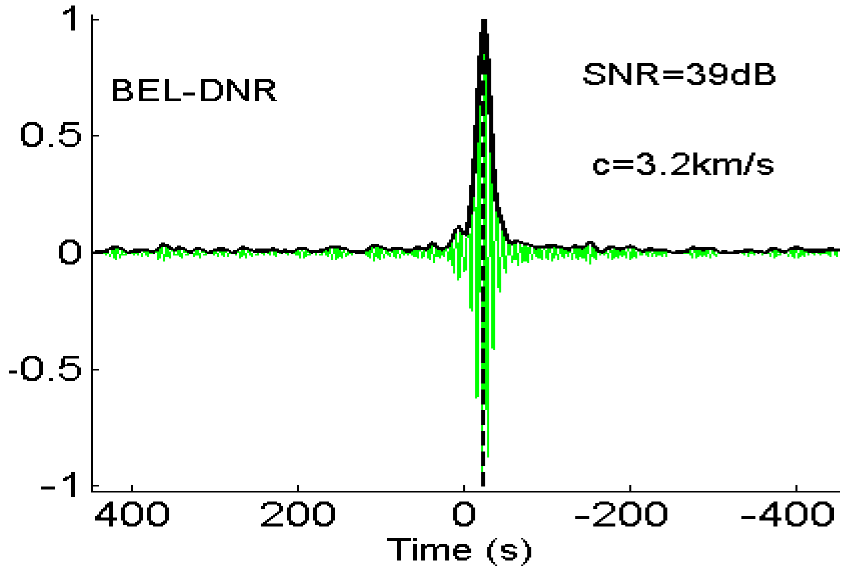

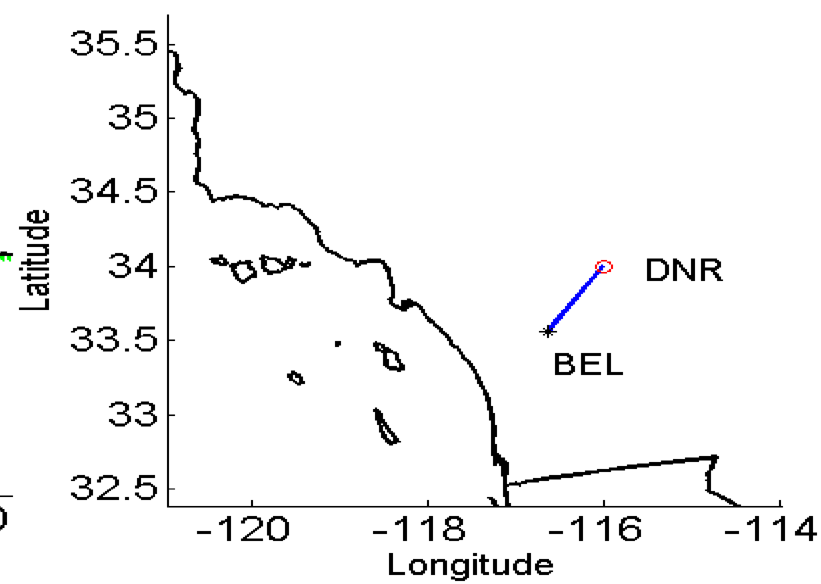

2D variations of the Rayleigh wave

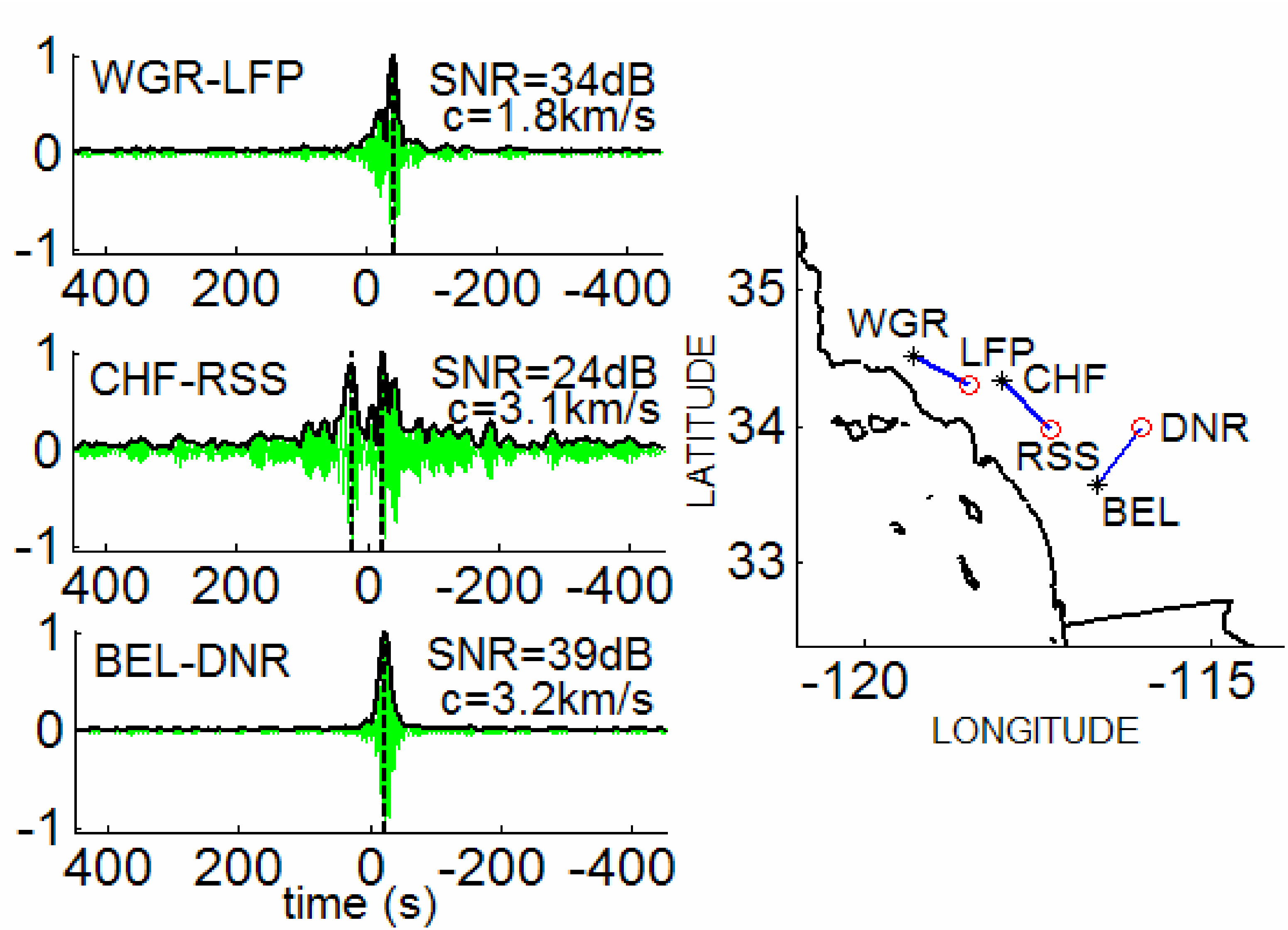

Surface wave Tomography 7.5s

TOMOGRAPHIC map

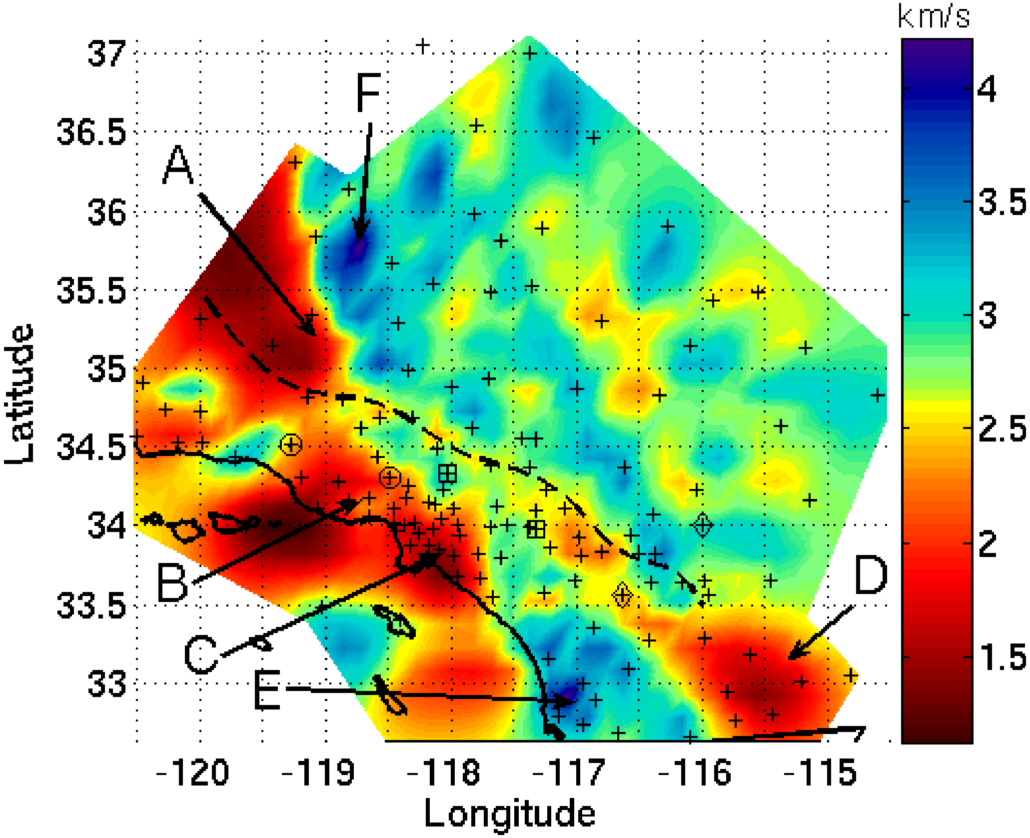

TOPOGRAPHIC map

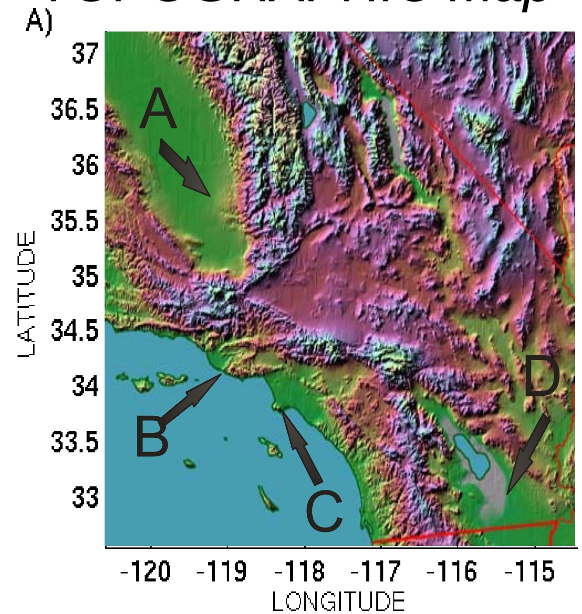

Grid 13*16km, uniform *a priori* velocity: c=2.8km/s. σ_T=2s, σ_c=0.15km/s(errors)

From 3D model, Kohler (2003)

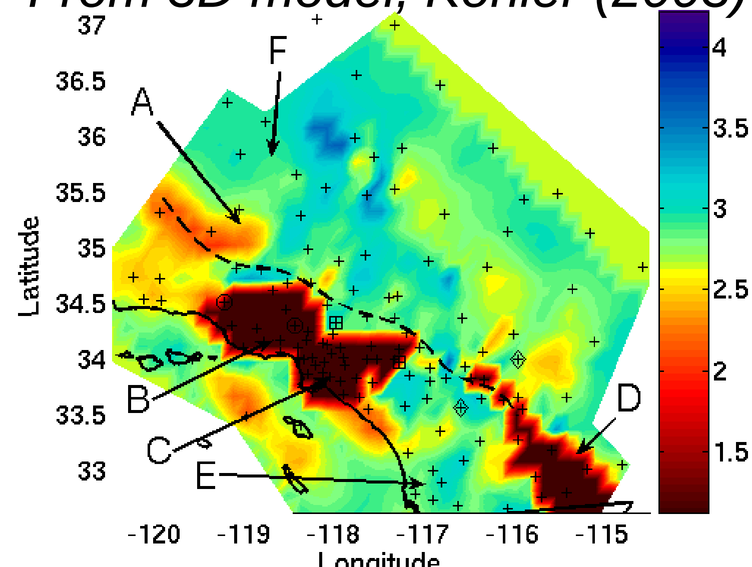

A: San Joaquin, B: Ventura, C: L.A., D: Salton Sea, E: Peninsular ranges, F: Sierra Nevada

Small scale geophysics inversion -in your backyard

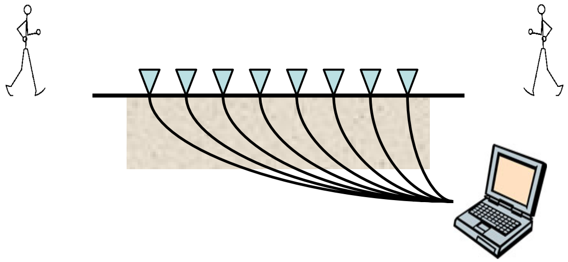

1-Cross-Correlations

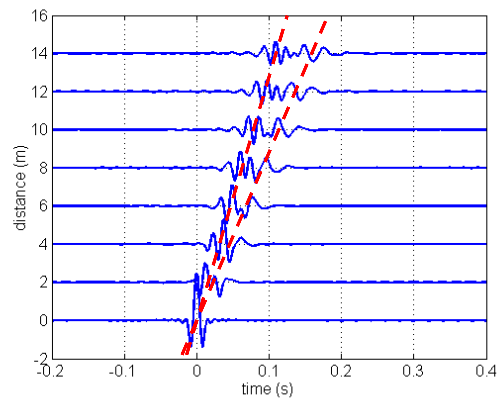

2-FK transform

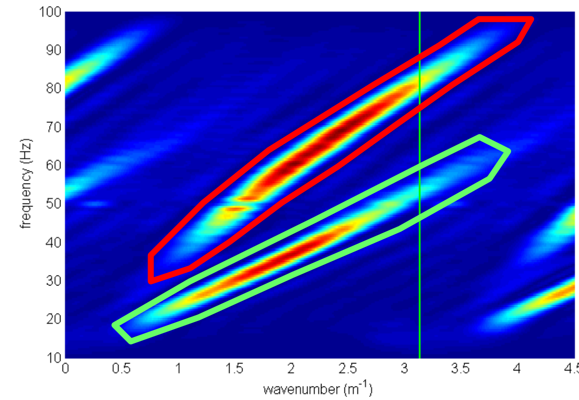

3-Extracting Rayleigh modes

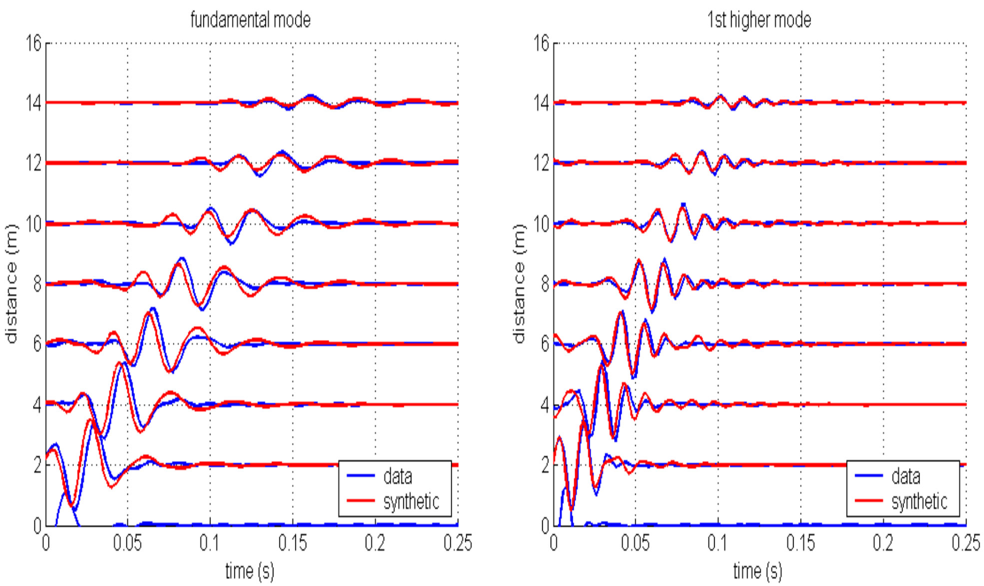

4-Inversion from dispersion curves

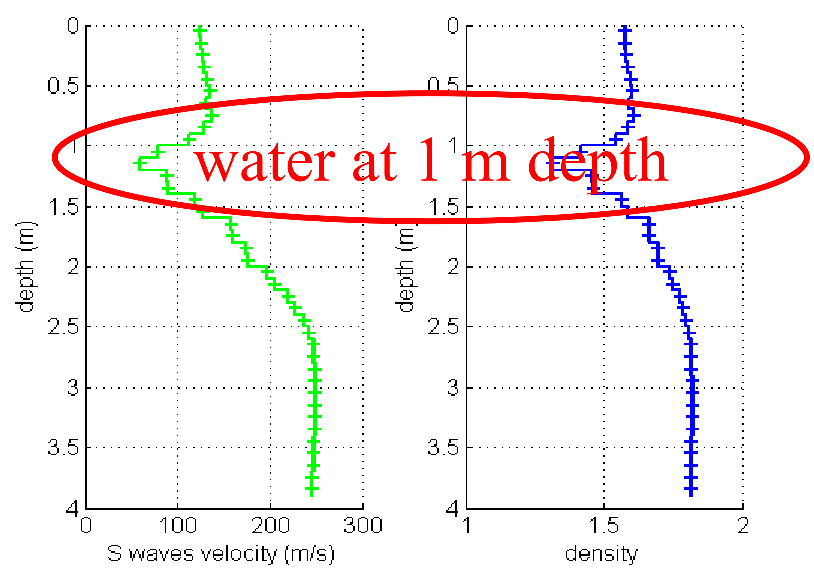

P. Gouédard, P. Roux and M. Campillo, LGIT, Grenoble, France

Cross-correlations of seismic noise *on the Moon* !

Seismic noise origin:
Thermal Cracks
(-170°C / +110 °C)

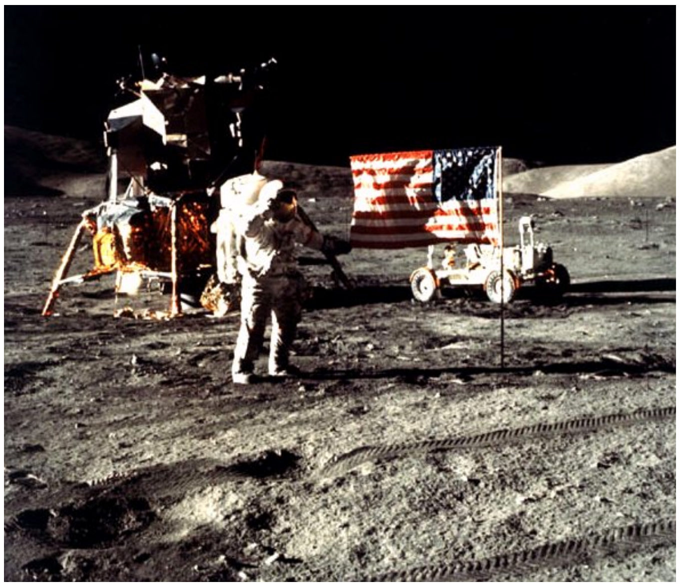

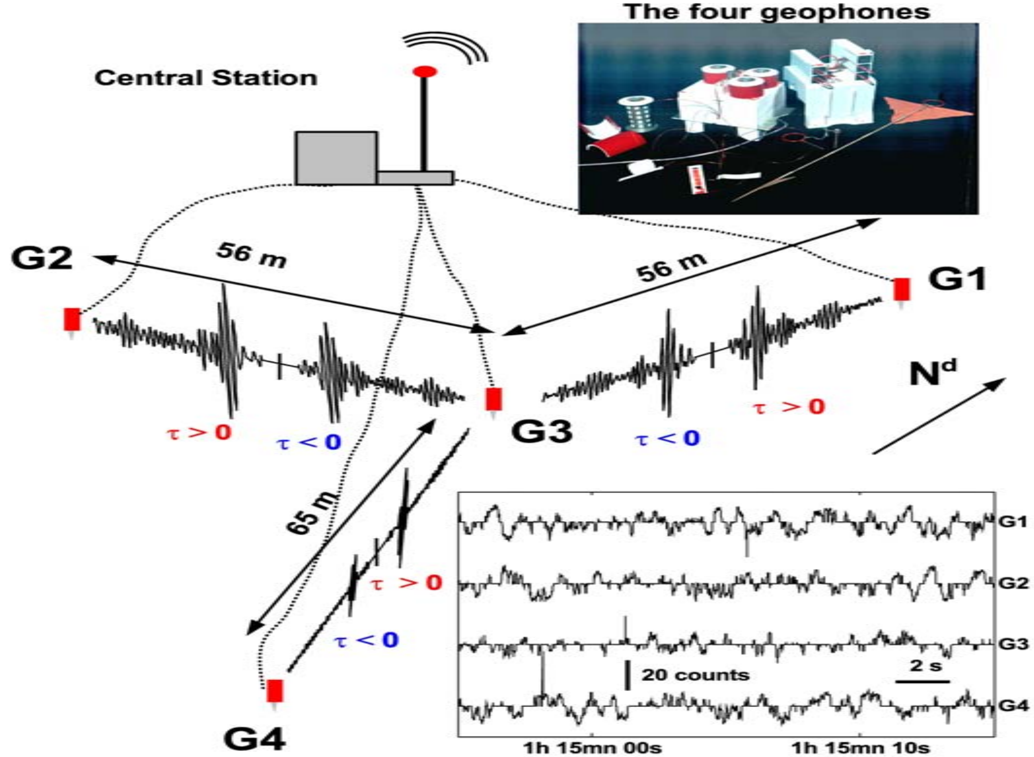

*Larose et al. ,Geophys. Res. Lett.,**32** (2005)*

Applications exist in a wide range of environments and frequency bands because the physics driving this noise cross-correlation process remains similar.

Using Structural Noise

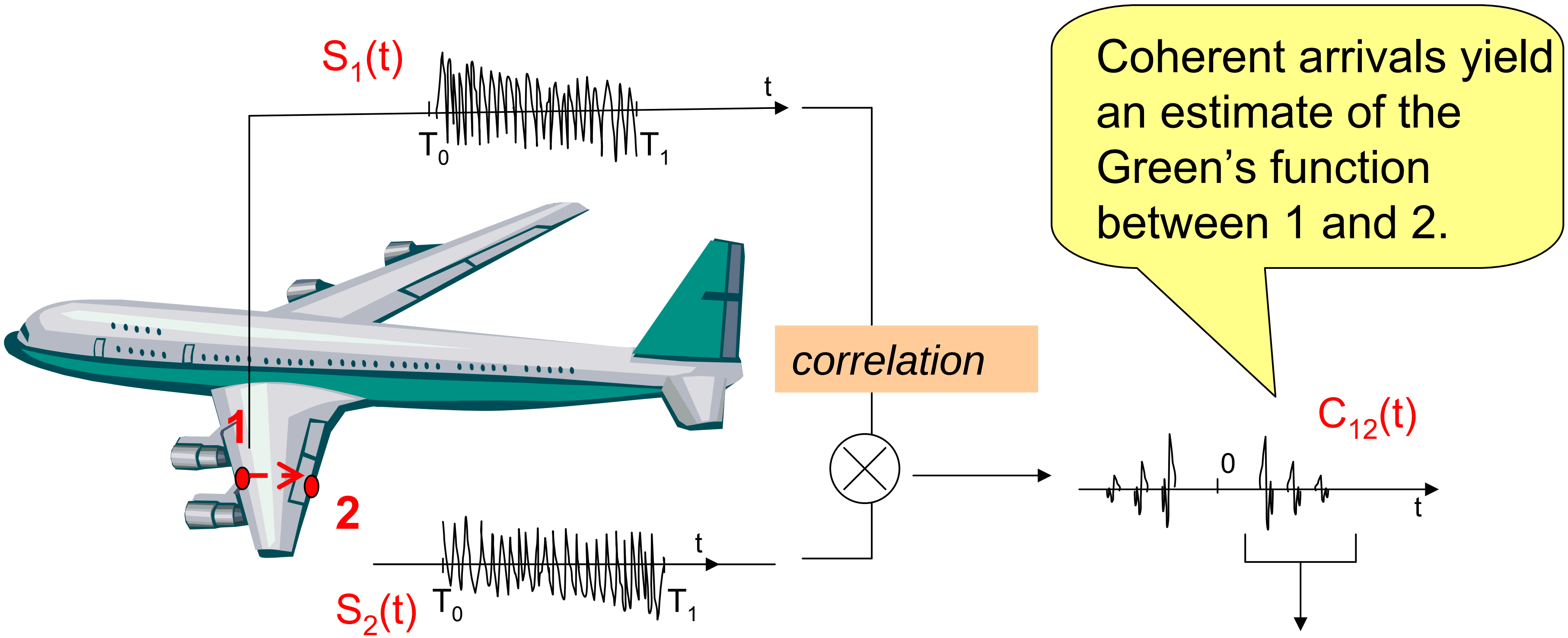

Acoustic and vibration waves that propagate through the locations of two receivers coherently average and dominate the cross-correlation function of the receiver pair for long time records.

SABRA ET AL (JASA: April 07)

Test Concept: Structural Health Monitoring of Pipeline Bases on Flow-Induced Vibrations

An oil pipeline

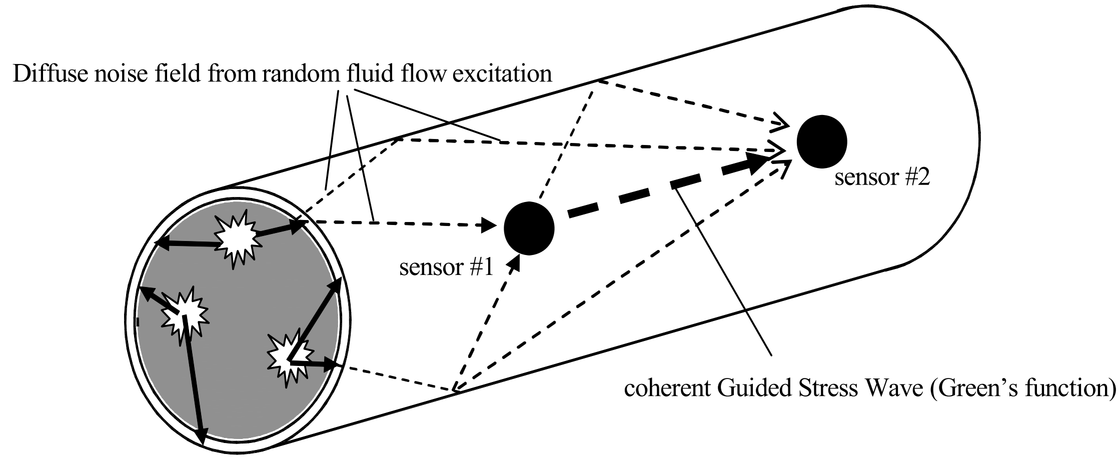

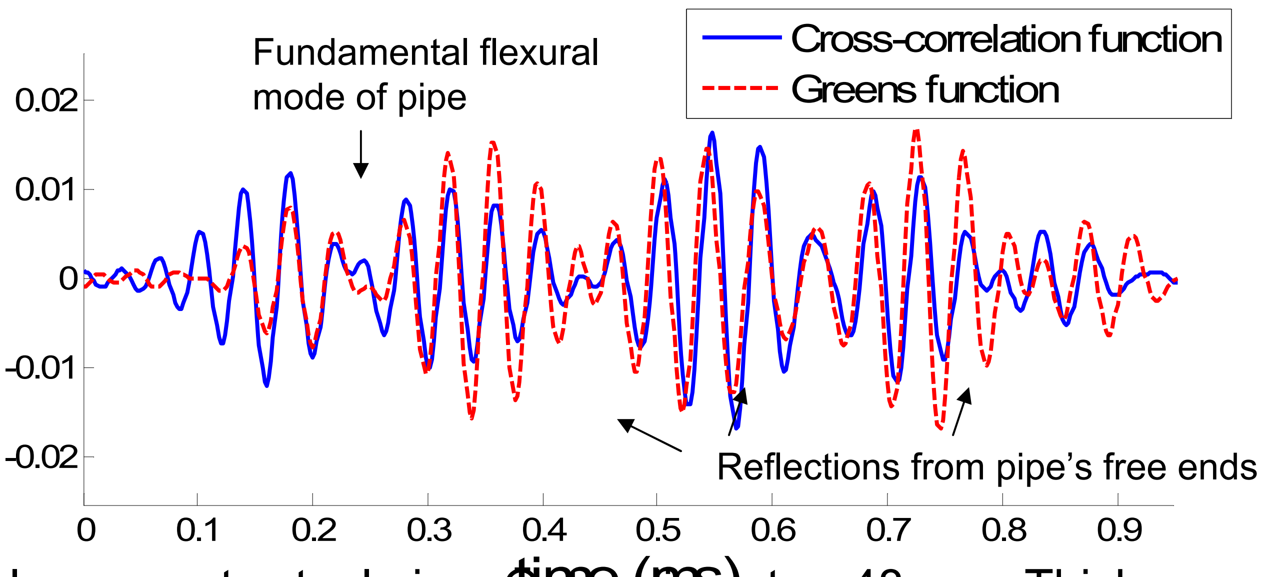

Noise sources =random laser excitations

965mm-long, empty steel pipe. Outer diameter=48 mm. Thickness=4.5 mm. [10-30kHz]

Experimental Set-up: Test Facility

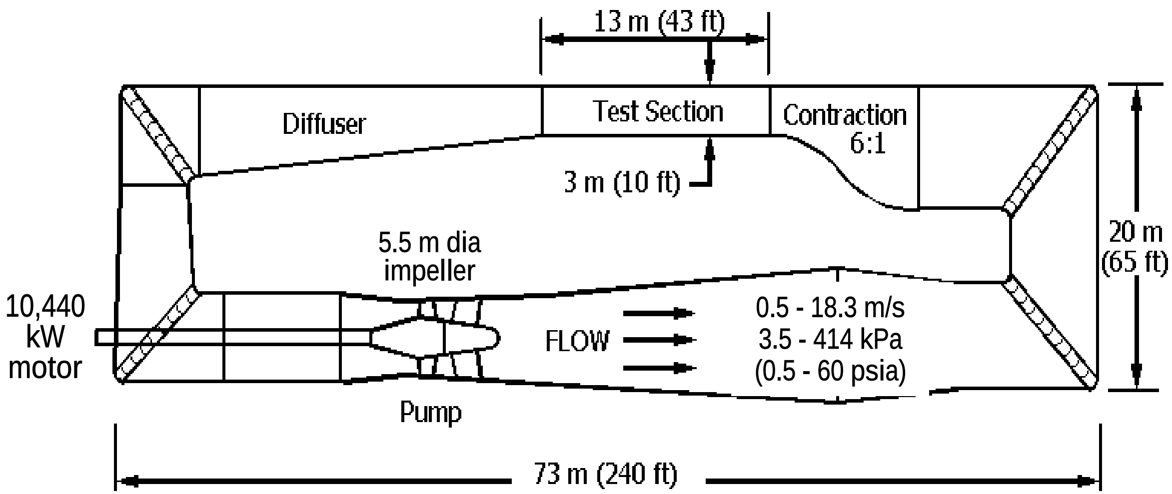

U.S. Navy's William B. Morgan Large Cavitation Channel, Memphis, TN

Test section & Hydrofoil Profile

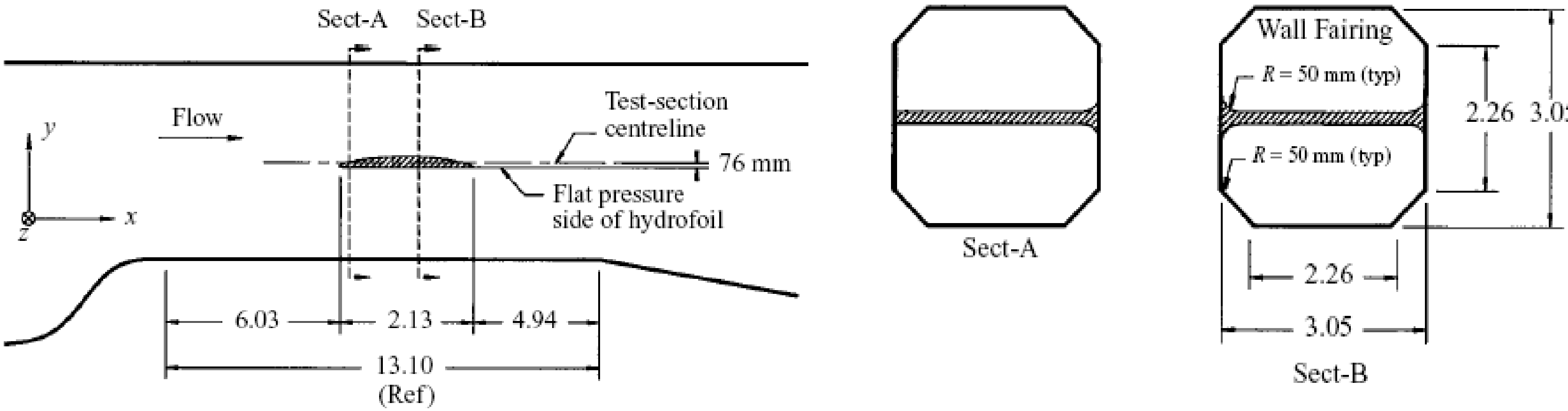

Flow Speed 18.3m/s. Chord-based Reynolds Number ~ 50 Million

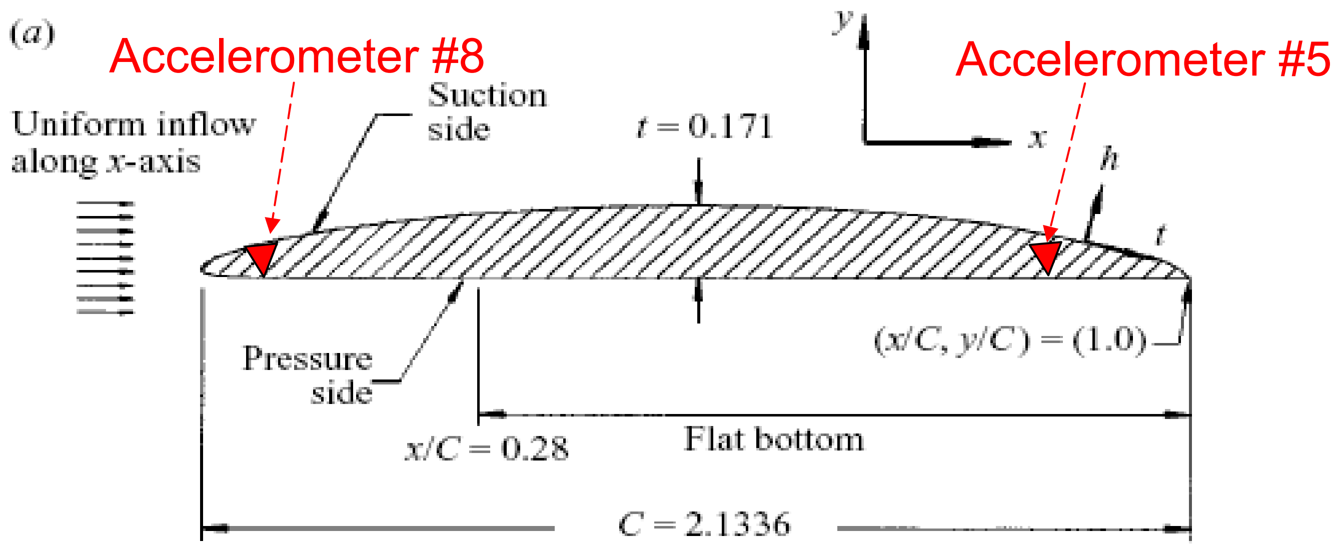

Figures reproduced from: Bourgoyne, et al. *JFM*, 2003.

Hydrofoil installed in the LCC

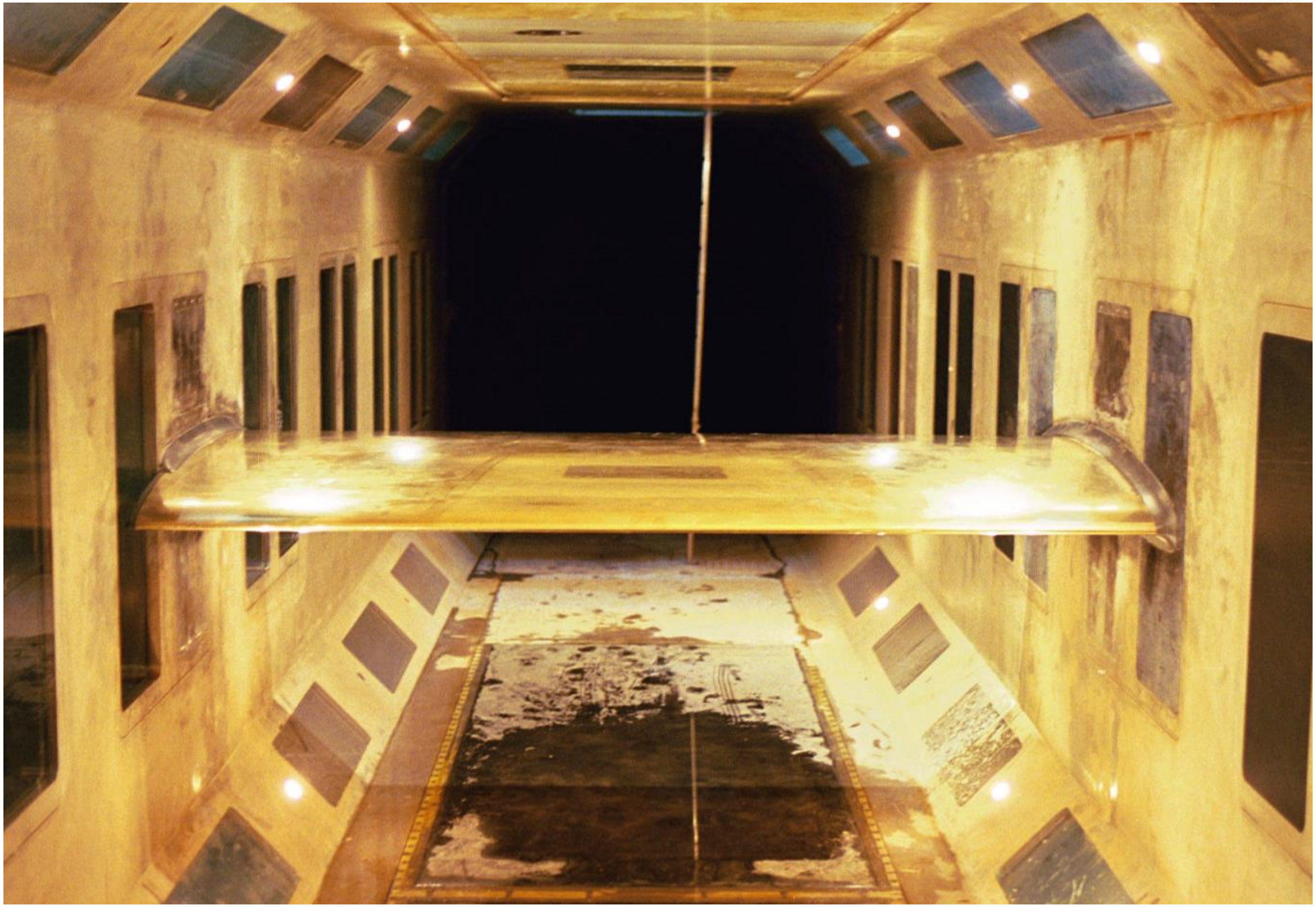

(view looking downstream)

Spectrum of random vibrations generated by the turbulent boundary layer

Sensor Separation, D=1.77m. Each Noise Recording duration=1 min.

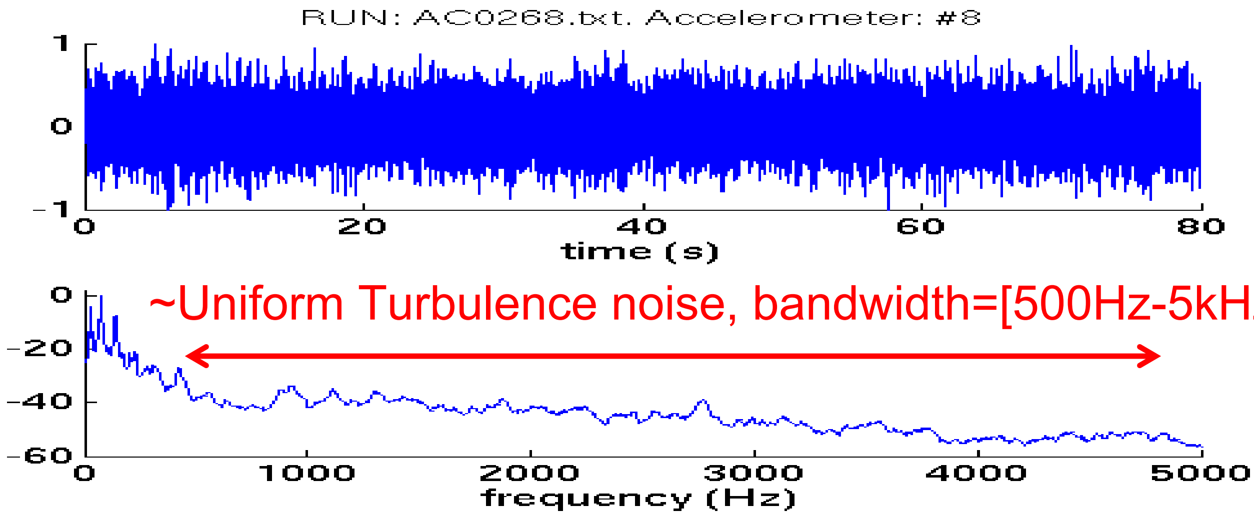

Accelerometer # 8

Leading Edge

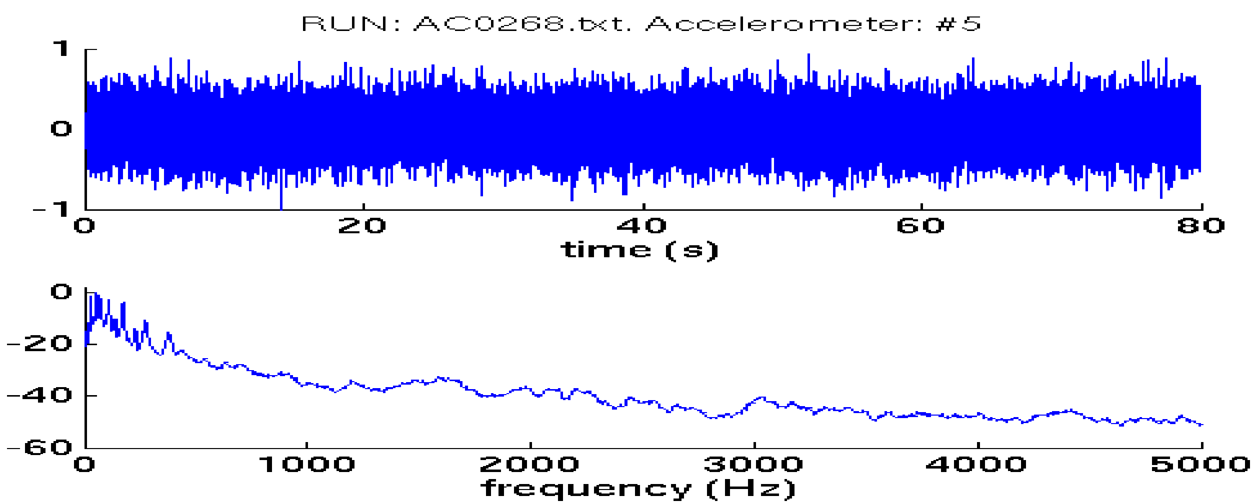

Accelerometer # 5

Trailing Edge

Cross-Correlation Function: Normal Mounting

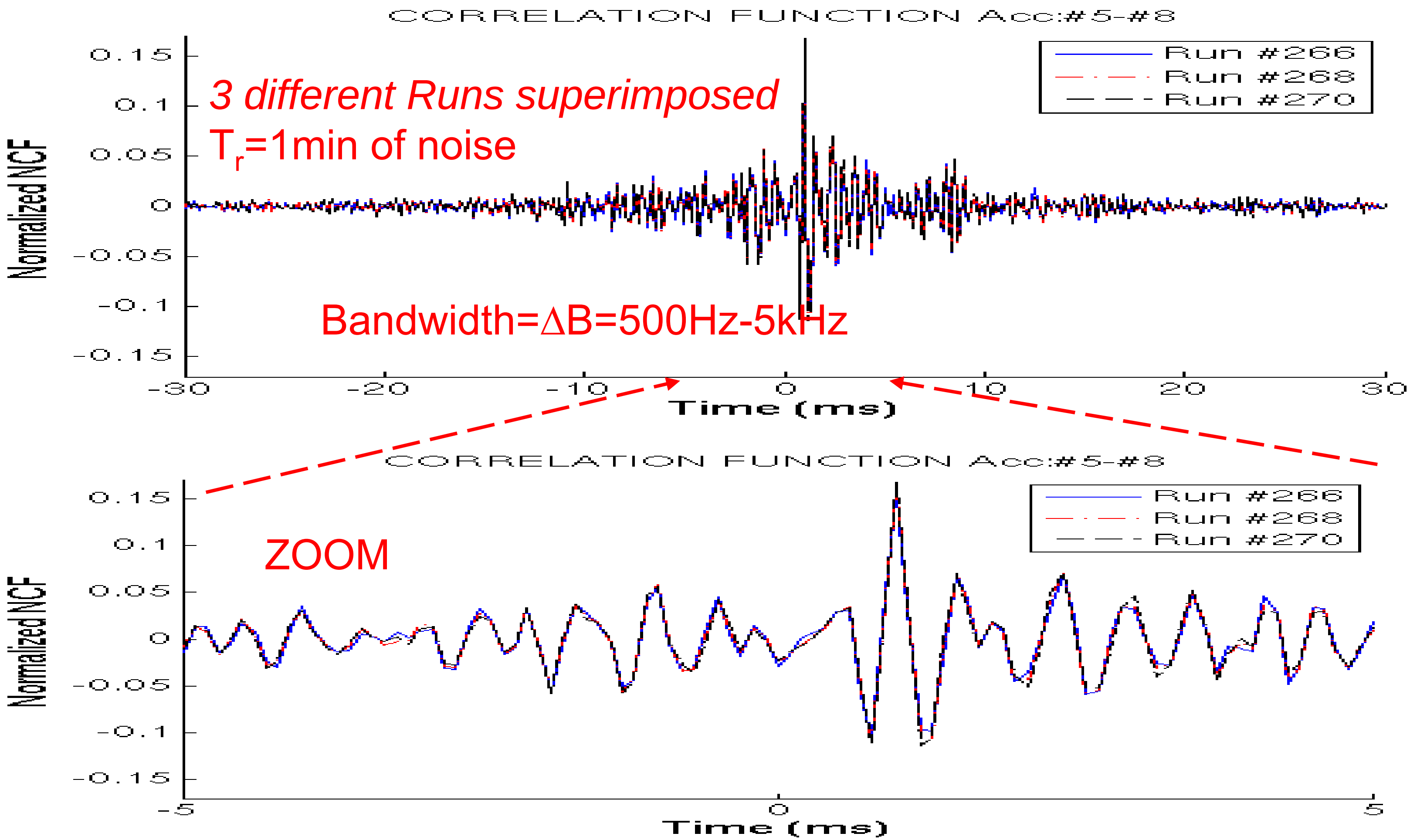

•Coherent and identical time-signatures emerge from the noise cross-correlation function between the accelerometer pair using three different recordings, T_r=1min. This time signature corresponds to the structural Green's function between the two accelerometer locations.

• Emergence rate of the coherent signature: **SNR≡ sqrt (T_rΔB)**

Cross-Correlation Function: Deformed Mounting

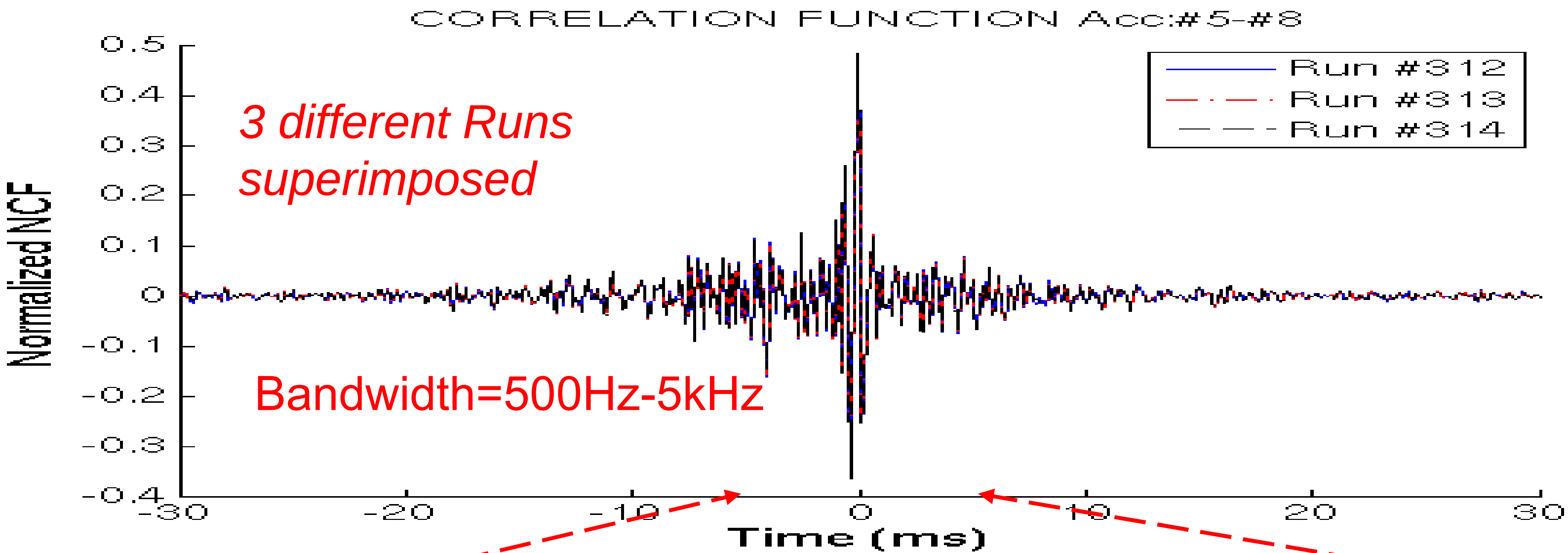

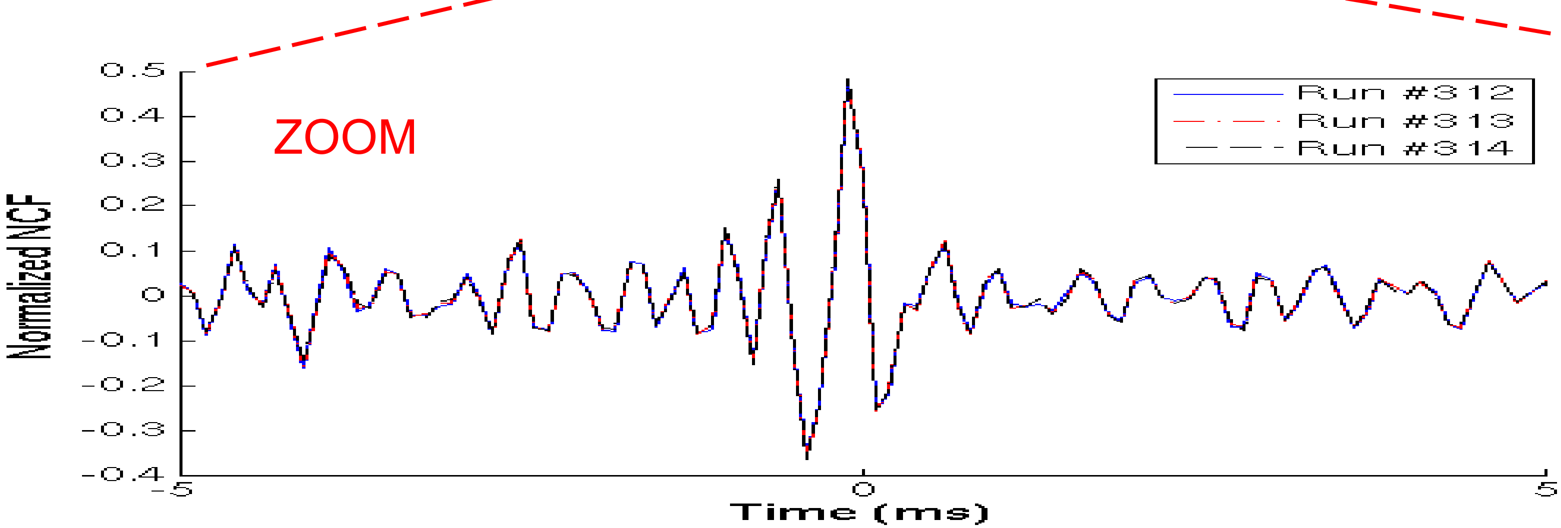

Again a consistent temporal signature of the noise cross-correlation function emerges, but it differs from the pre-cavitation test signature.

Monitoring Structural Changes

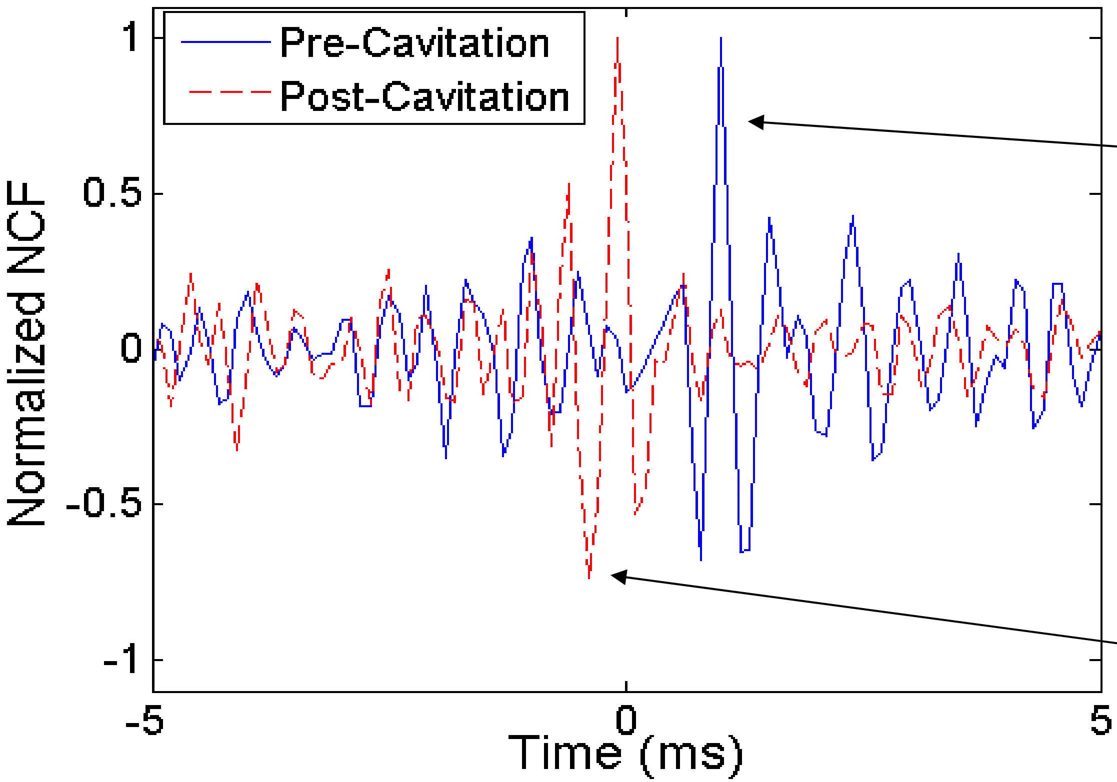

Normal Mounting

BEFORE Cavitation tests

Deformed Mounting

AFTER cavitation tests

Variations in the temporal structure of the noise cross-correlation function reveals that structural changes in the hydrofoil and its mounting have occurred because of the short-but-intense cavitation tests (Deformed Mounting was nearly equidistant from the two accelerometers).

Muscle Noise

In 1810, the British physicist, physician and chemist, William Hyde Wollaston, compared the muscle sounds to the distant rumble of carriages over the cobblestone streets of London. To check his work, he had his carriage driven through the streets at various speeds until the noise matched the rumbling he heard through his thumbs.

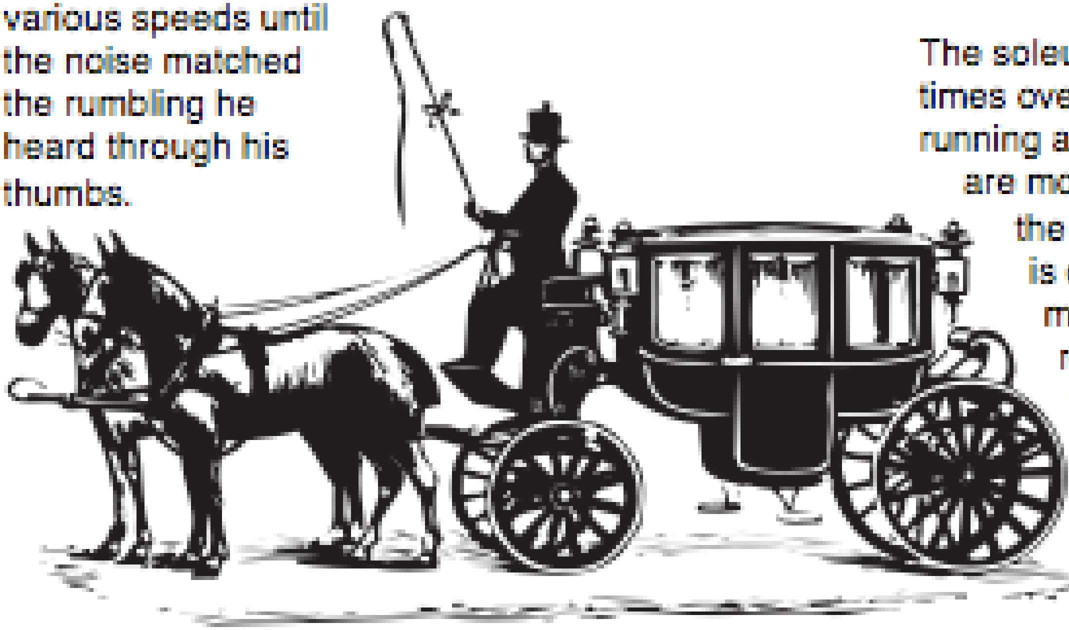

Knowing the size of the cobblestones, and the wheel diameter, he was able to calculate the muscle sounds to be about 25 Hertz.

This fact i
sounds ca
muscle is
the least s
angle betw
115 degre

The soleus
times over
running an
are mor
the r
is c
mu
re

Muscle fi
twitch" fib
can contr
twitch fibe

Partial History of the Fourier Transform

Horse-Spectrometer (1810)

Fourier (1810): published in 1822

.

.

Passive in-vivo Elastography from skeletal muscle noise

Karim G. Sabra, Stephane Conti,

Philippe Roux, William A. Kuperman

Marine Physical Laboratory, Scripps, UCSD

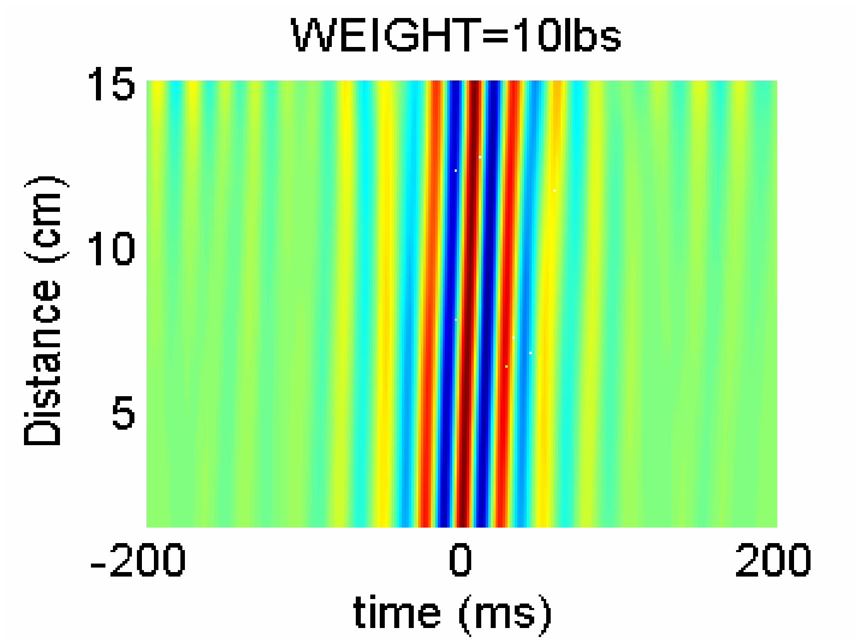

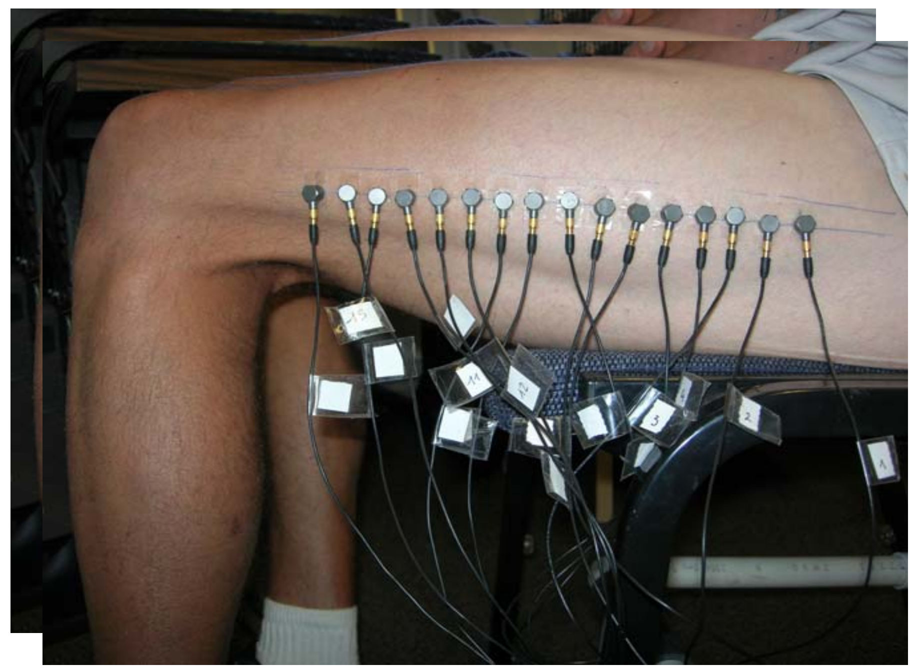

Elastic Properties of Tissues

$$E = \frac{\sigma}{\varepsilon}$$

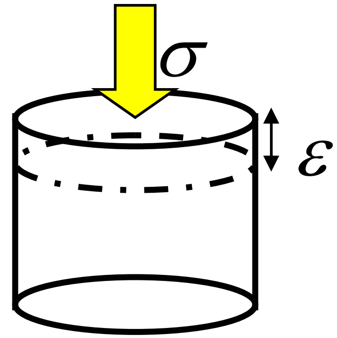

$$E = \mu \frac{3\lambda + 2\mu}{\lambda + \mu} \approx 3\,\mu$$

λ et μ Lamé coefficients

Biological Tissues : λ = 2,5 GPa, μ = 25 kPa

Human Body

H.F. (1-50 MHz)

Fluid (Compressionnal waves)

-sound speed slight changes ~ 1500 $m.s^{-1}$

- Echogeneicity imaging $Z = \rho c$

$$c = \sqrt{\frac{\lambda + 2\mu}{\rho}} \approx \sqrt{\frac{\lambda}{\rho}}$$

B.F. (1-100Hz)

Elastic Solid (Compression + Shear waves)

- Shear wave speed is slow ~ 1-5 $m.s^{-1}$

- centimetric wavelengths

$$v = \sqrt{\frac{\mu}{\rho}}$$

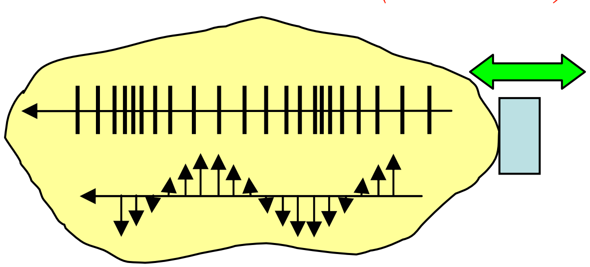

MechanoMyoGrams (MMG)

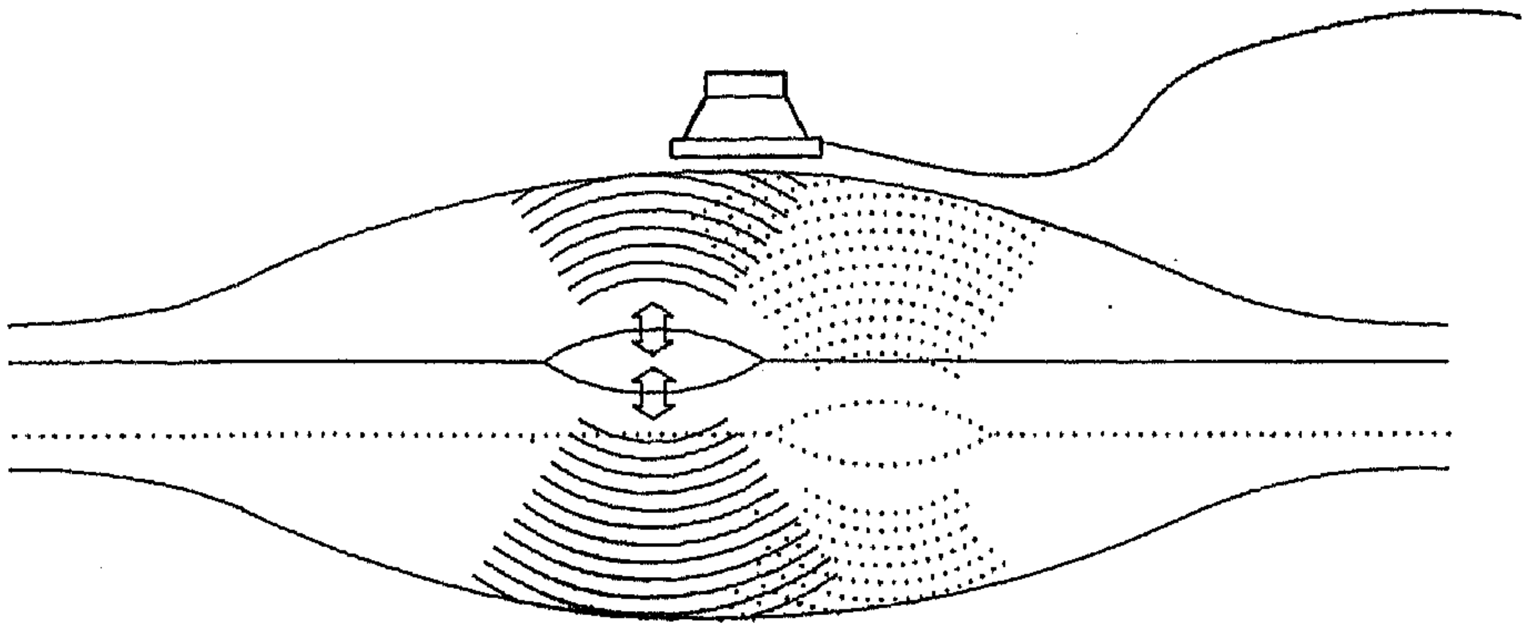

Figure 11.3. Schematic representation of the hypothesised MMG generation process.

MMG result from vibrations generated by dimensional changes of the active muscle fibers during (fluctuations of) voluntary contractions (*Orizzio 93*)

→ *Are shear waves generated naturally ?*

Motivation

Shear wave excitation techniques used in active elastography

ACTIVE

- Elastography
  - Static excitation
    - *Ophir, Bertrand*
  - Dynamic excitation
    - Continuous wave (poly or mono-chromatic)
      - *Sato, Levinson, Parker, Greenleaf, Sinkus*
    - Pulsed wave
      - *Fink*

PASSIVE

Use random-vibrations generated by the human body itself (e.g. muscle twitches)

Shear speed measurement techniques

ACTIVE

- Shear speed measurement
  - Electromagnetic waves (RMN)
    - *Greenleaf, Sinkus*
  - Ultrasound
    - Intercorrelation
      - *Fink, Ophir*
    - Doppler
      - *Sato, Levinson, Parker*

PASSIVE

"Surface mechanomyograms" using skin-mounted accelerometers

Extracting Green’s Function from Diffuse Wavefields

ACTIVE

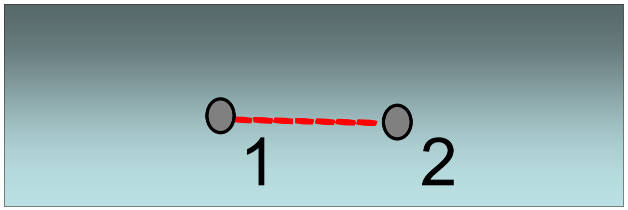

Sensor 1 broadcasts. Sensor 2 records.

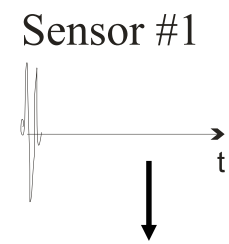

Active transmission

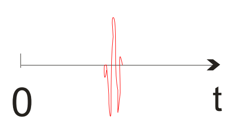

1→2

Green’s Function (- - -)

PASSIVE

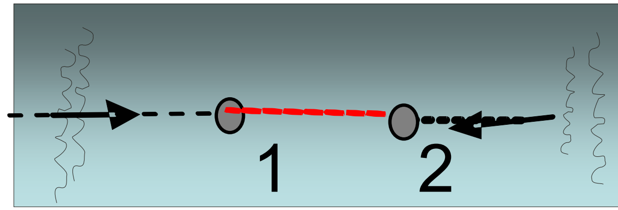

Diffuse field recorded at sensors 1 & 2.

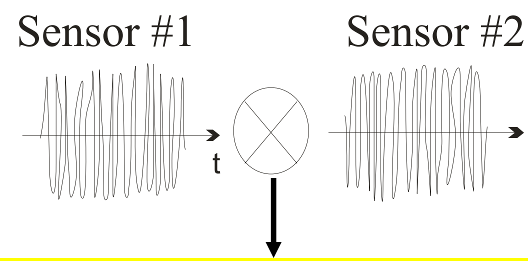

Cross-correlation between 1 and 2

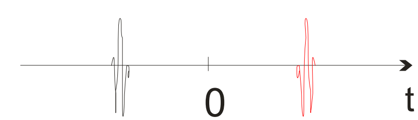

2→1 1→2

Green’s Function Estimate (- - -)

$$C_{12}(\tau) = \int_{-\infty}^{\infty} P(\mathbf{r}_1, t)\, P(\mathbf{r}_2, t+\tau)\,\mathrm{d}\,t.$$

Theoretical & Practical Issues

Formal relationship for diffuse fields cross-correlations:

$$C_{12}(\omega)=\beta\, Imag(G_{12}(\omega))= \beta\, (G_{12}(\omega)- G^*_{12}(\omega))/2i$$

Limiting Factors:

1. Distribution
2. Directionality
3. Power spectrum
4. Statistics

} due to the noise sources

5. Attenuation
6. Coherence length/duration

} due to the medium

$$T_{dispersion}<T_{statistical}<T_{recording}< T_{fluctuation}$$

On short time-scale ($< T_{fluctuation}$), the cross-correlation process is stationary

Experimental Set-up

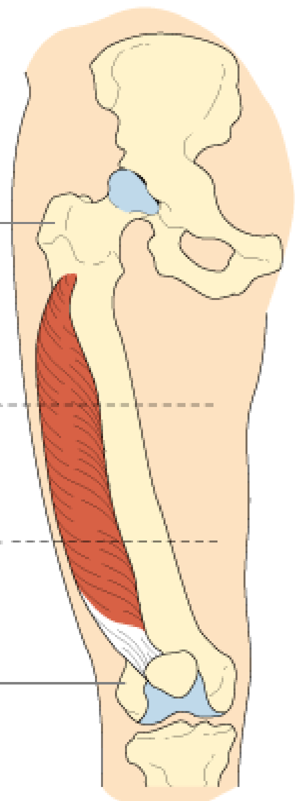

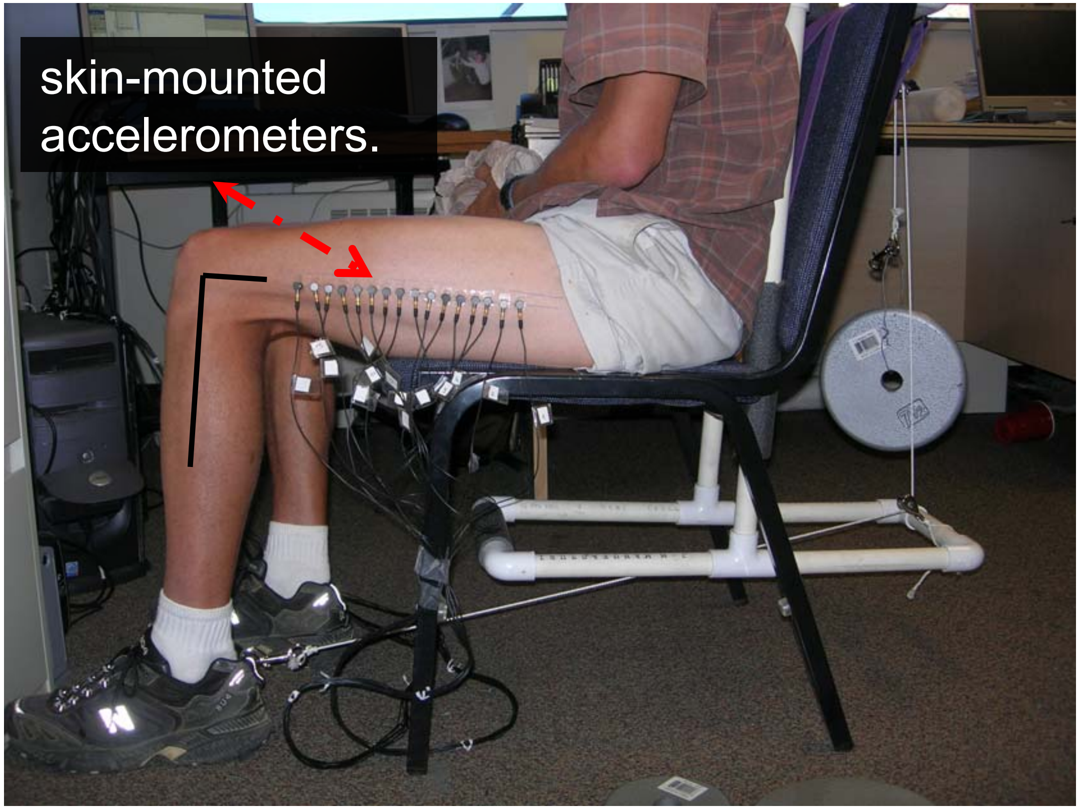

Miniature (1.5 gm), ceramic shear ICP® accel., 100 mV/g,

- <u>Method</u>: Isometric contractions of the vastus lateralis (knee extensor) muscle

- <u>Goal</u>: Relate “muscle hardness” (shear modulus) to weight load (produced effort/torque)

Surface Mechanomyograms (MMG)

Lifted weight= 10lbs

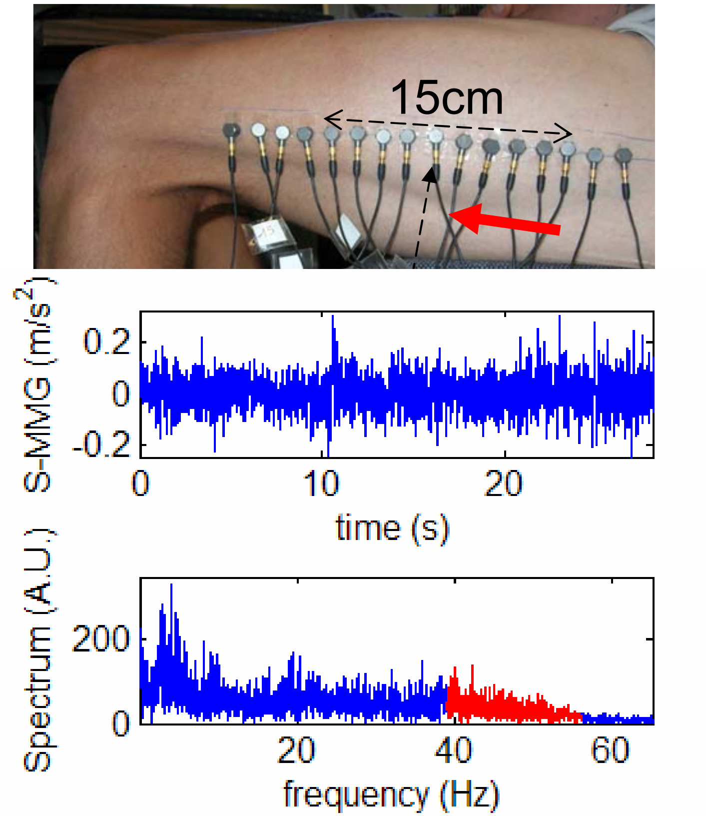

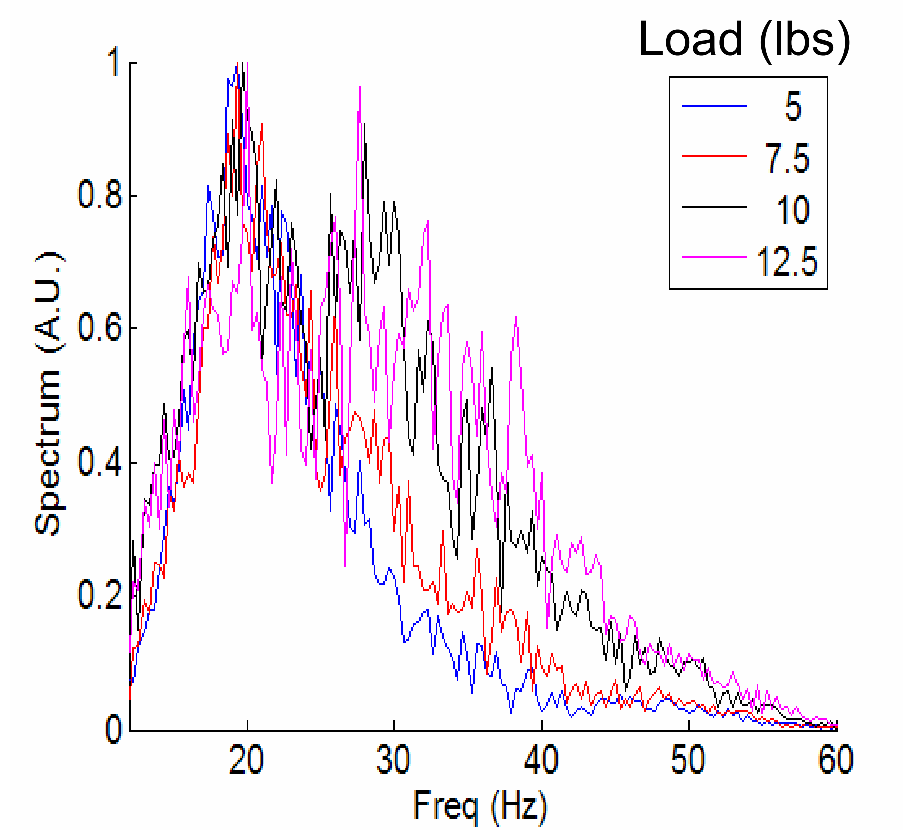

Spectral shift towards higher frequencies & increase of “rms” value with increasing effort due to:

1. Recruitment of faster motor units
2. Increase in firing rates of motor units (*Shinoara,98*)

Emergence of Coherent Shear Waves

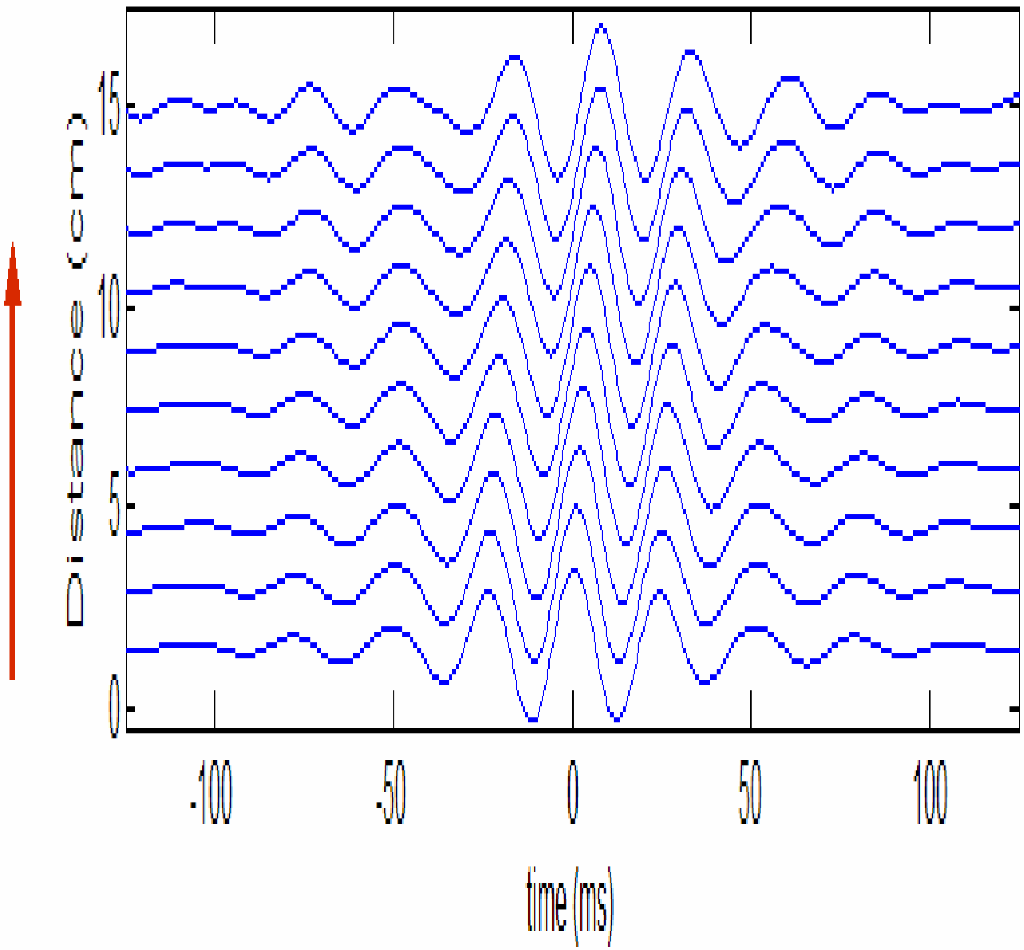

Sensor #1.

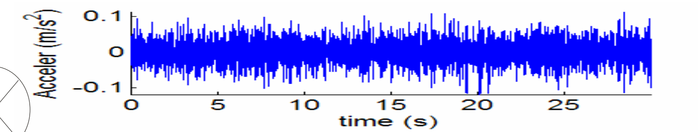

Sensor #11.

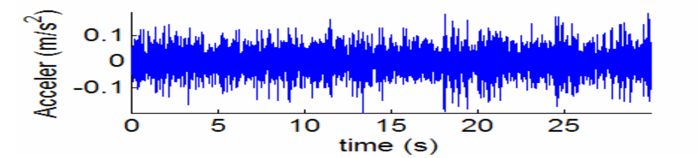

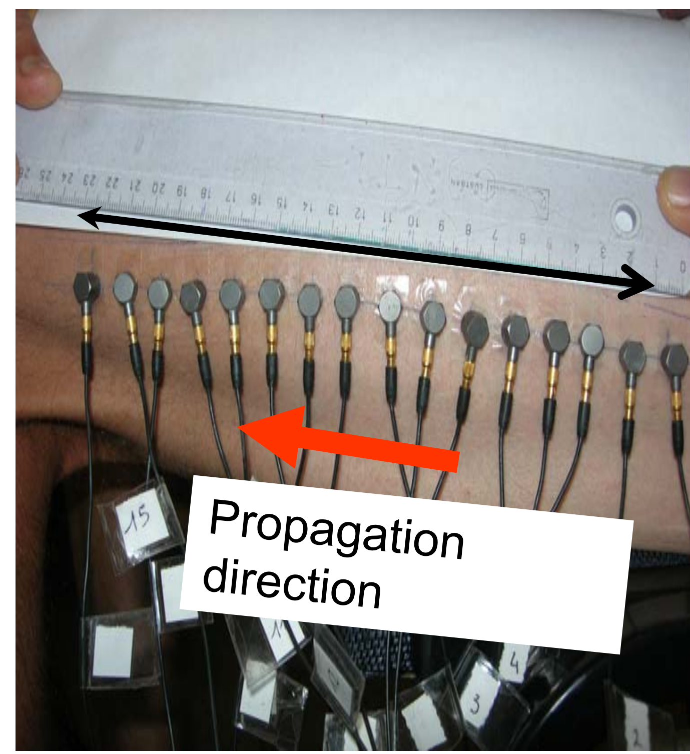

Weight=10lbs. Bω=[40Hz-55Hz].
30sec of muscle noise

Coherent Shear Wave Profile

Average profile over all equidistant pairs

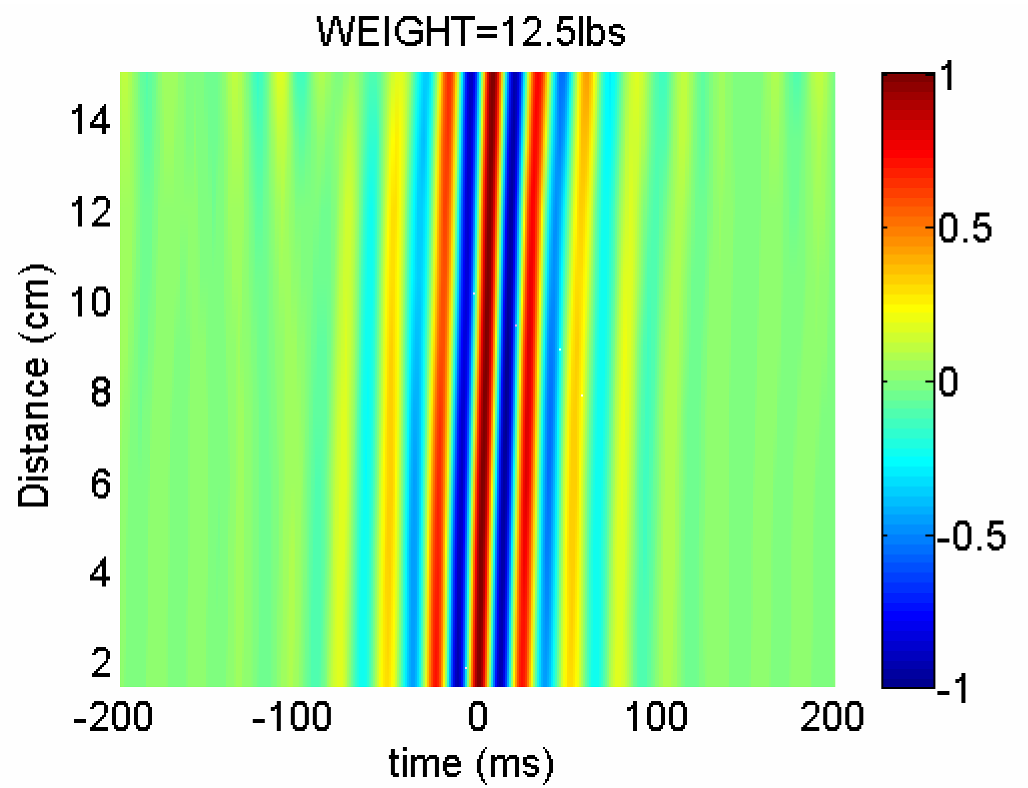

Bω=[40Hz-55Hz]

•Only use sensors mounted on the middle third of the vastus lateralis muscle

•Pennation angle~5degrees. *[Winter, 1990]*

Shear Wave Speed Dispersion

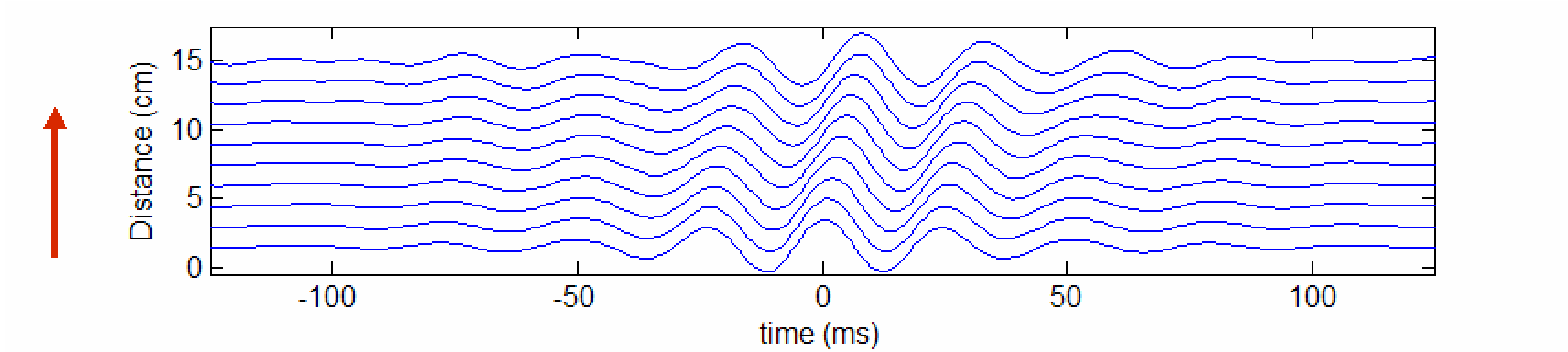

Voigt model

$$-\rho\omega^2 S = (\mu_1 + i\omega\mu_2)\Delta S$$

μ_1 : Shear modulus (kPa)

μ_2 : Shear viscosity (Pa.s)

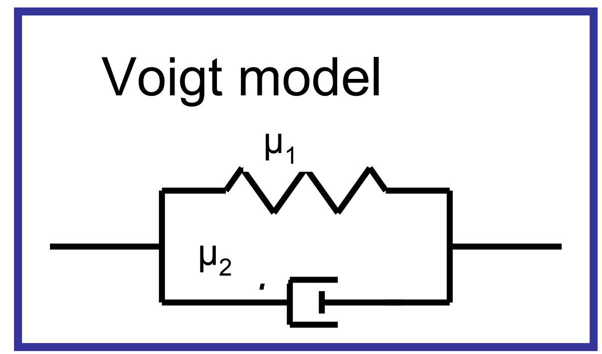

$$k = \sqrt{\frac{\rho\omega^2}{\mu_1 + i\omega\mu_2}} \longrightarrow c_s = \sqrt{\frac{2(\mu_1^2 + \omega^2\mu_2^2)}{\rho\left(\mu_1 + \sqrt{\mu_1^2 + \omega^2\mu_2^2}\right)}}$$

For isotropic elastic (small displacement), locally homogeneous tissue

Viscoelastic parameters vs. load

Voigt model $$c_s = \sqrt{\frac{2\left(\mu_1^2 + \omega^2 \mu_2^2\right)}{\rho\left(\mu_1 + \sqrt{\mu_1^2 + \omega^2 \mu_2^2}\right)}}$$

μ_1 : Shear modulus (kPa),

μ_2 : Shear viscosity (Pa.s),

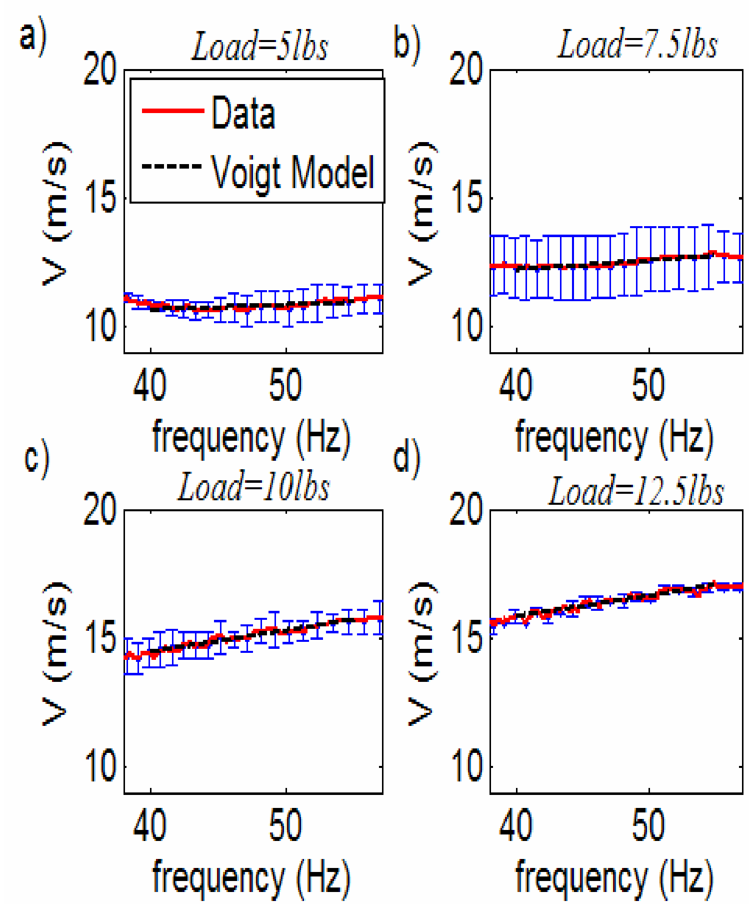

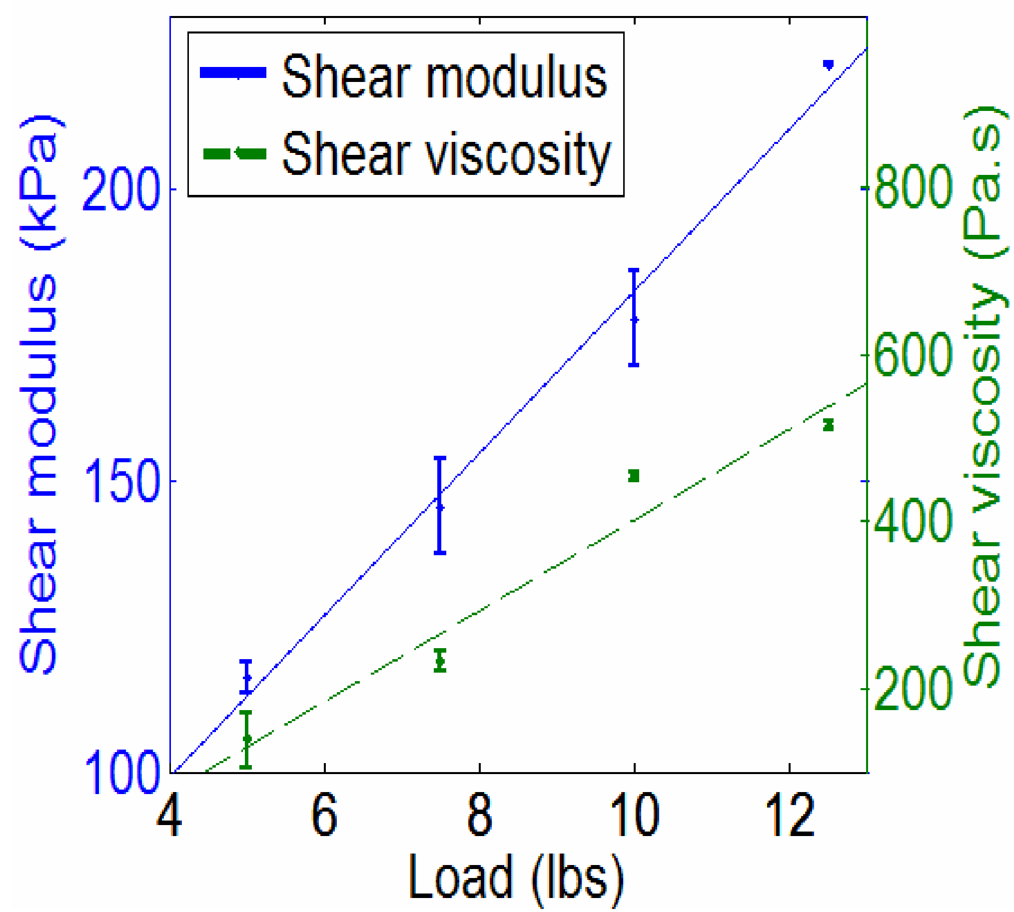

Conclusions

- AMBIENT NOISE IS NOT ALWAYS A NUISANCE
- SOMETIMES THE NOISE IS THE SIGNAL
- COHERENT STRUCTURES CAN BE BUILT UP FROM NOISE CORRELATION
    - The time-bandwdith product of the recordings governs the accuracy of the results: SNR$\equiv$ sqrt ($T_r \Delta B$).

NOISE CAN BE

- USED FOR INVERSION
- USED FOR NON DESTRUCTIVE TESTING
- USED FOR IN SITU MONITORING OF STRUCTURES
- USED FOR PASSIVE MONITORING OF HUMAN BODY
- CAN BE ADDED FOR DETECTION OF WEAK SIGNAL
-